U.S. DEPARTMENT OF THE INTERIOR

U.S. GEOLOGICAL SURVEY

# Geologic map of the Hamilton Buttes quadrangle, southern Cascade Range, Washington

by

Donald A. Swanson[1]

Open-File Report 96–0016



[1]U.S. Geological Survey, University of Washington, Department of Geological Sciences, Box 351310, Seattle, Washington 98195-1310

## CONTENTS



### FIGURES



### TABLES



### PLATES

# Geologic map of the Hamilton Buttes quadrangle, southern Washington Cascade Range

by Donald A. Swanson

## INTRODUCTION

The Hamilton Buttes 7.5–minute quadrangle is centered about 60 km northeast of Mount St. Helens, 25 km north-northwest of Mount Adams, and 10 km west of the crest of the Cascade Range in southern Washington (fig. 1). It is the most recent in a series of adjoining quadrangles that I have studied geologically. Geologic maps and accompanying detailed text have been open-filed for the French Butte, Greenhorn Buttes, Tower Rock, McCoy Peak, Blue Lake, and East Canyon Ridge quadrangles (Swanson, 1989, 1991, 1992, 1993, 1994a). In addition, I mapped that part of the Randle quadrangle south of the Cowlitz River (Moore and others, 1994). I have also finished mapping those parts of the Purcell Mtn. and Packwood quadrangles south of the Cowlitz River (D.A. Swanson, unpublished mapping, 1994); this mapping will be combined with that by R.B. Moore and N.G. Banks north of the Cowlitz. In 1995 I completed mapping the Packwood Lake quadrangle.

The geologic research in these quadrangles forms part of an effort, which began small but over the years has become a major undertaking, to understand the development of the Cascade arc in southern Washington from its inception in the late Eocene. A primary goal has been to tie the Tertiary stratigraphy of the area near and west of Mount St. Helens (Evarts and Ashley, 1984, 1990a, b, 1991, 1992, 1993a, b, c, d; Evarts and others, 1987; Swanson, 1989, 1991, 1992, 1993, 1994a) into the now classic stratigraphic section in the Mount Rainier–White Pass area defined by Fiske and others (1963; see also Waters, 1961) and modified by Vance and others (1987). This work is establishing an improved regional geologic framework for the southern Washington Cascades and defining a geologic research corridor across the west side of the Cascade Range (Swanson and Evarts, 1992; Evarts and Swanson, 1994), from the upper Eocene marine rocks of the Puget Lowland to the Late Jurassic–Early Cretaceous Rimrock Lake inlier (Miller, 1989; Miller and others, 1993) along and just east of the crest in the White Pass–upper Tieton River area and eastward to the margin of the Columbia Plateau (Swanson, 1978) (fig. 1). The ongoing study will provide geologic support for a seismic refraction and reflection study (conducted in late summer 1995) and other geophysical surveys in a corridor linking coastal Washington with the Columbia Plateau (Wells and others, 1993). Detailed field work is testing whether a pronounced electrical conductivity layer in the middle crust, the *southern Washington Cascades conductor* (SWCC) of Stanley and others (1987, 1992), has a recognizable influence on the geology of the area. All of the quadrangles that I have studied lie either within the SWCC or astride its margin.

Most of the Hamilton Buttes quadrangle drains into the Cispus River (fig. 2), a trunk stream carrying water from the north side of Mount Adams and the southwest side of the Goat Rocks Wilderness westward into the Cowlitz River. The northern part of the quadrangle drains into the Cowlitz via northwest-flowing Johnson Creek and its tributaries.

Roads follow most major drainages in the quadrangle, and logging roads (a few not shown on the quadrangle map) in various conditions climb some steep slopes. Access is by foot trail in the northeastern part of the quadrangle (in the Goat Rocks Wilderness), along Elk Ridge, and along the divide from St. John Lake past Mission Mountain and south beyond Point 5288 (fig. 2). Shorter trails enable easy access to the south side of Hamilton Buttes, the ridge between Hugo Lake and Chambers Lake, and the Cispus River just below Mile 47. Rugged Stonewall Ridge and upper Mission Creek have neither roads nor trails. Some trails are not shown on the quadrangle. Also note that the boundary of the Goat Rocks Wilderness is incorrect on the quadrangle; in particular the Wilderness has been extended north and east of Chambers Lake.

Late Eocene, Oligocene, and early Miocene volcaniclastic and volcanic rocks, mainly of basaltic andesite and andesite composition (table 1), underlie most of the quadrangle. Volcaniclastic rocks greatly predominate and compose what previous workers in the quadrangle have called the Ohanapecosh Formation (Hammond, 1980; Swanson and Clayton, 1983; Winters, 1984; Stine, 1987; Korosec, 1987). Fluvial micaceous arkose and mudstone are interbedded and mixed with the lower part of the volcaniclastic section (Winters, 1984; Swanson, 1994b). Many intrusions, mostly sill-like and generally basaltic andesite or andesite, cut the layered rocks. Pleistocene basalt, andesite, and dacite flows underlie much of the eastern part of the quadrangle. Most of the lava flows were erupted from vents east of the quadrangle, but flows of andesite and dacite on Goat Ridge apparently have a local source. A subglacial volcano lies just east of the quadrangle.

Glacial drift covers large areas, but generally bedrock crops out along creeks, steep slopes, and ridges. The bedrock mapping involved traverses along most drainages, large and small; such work finds many exposures, even in densely forested terrain.

Previous small-scale (1:100,000 and smaller) reconnaissance geologic mapping has included the Hamilton Buttes quadrangle, mainly by Hammond (1980), Korosec (1987), and Smith (1993). Winters' (1984) thesis study of the arkose includes a 1:24,000 scale map and cross sections of part of the area.

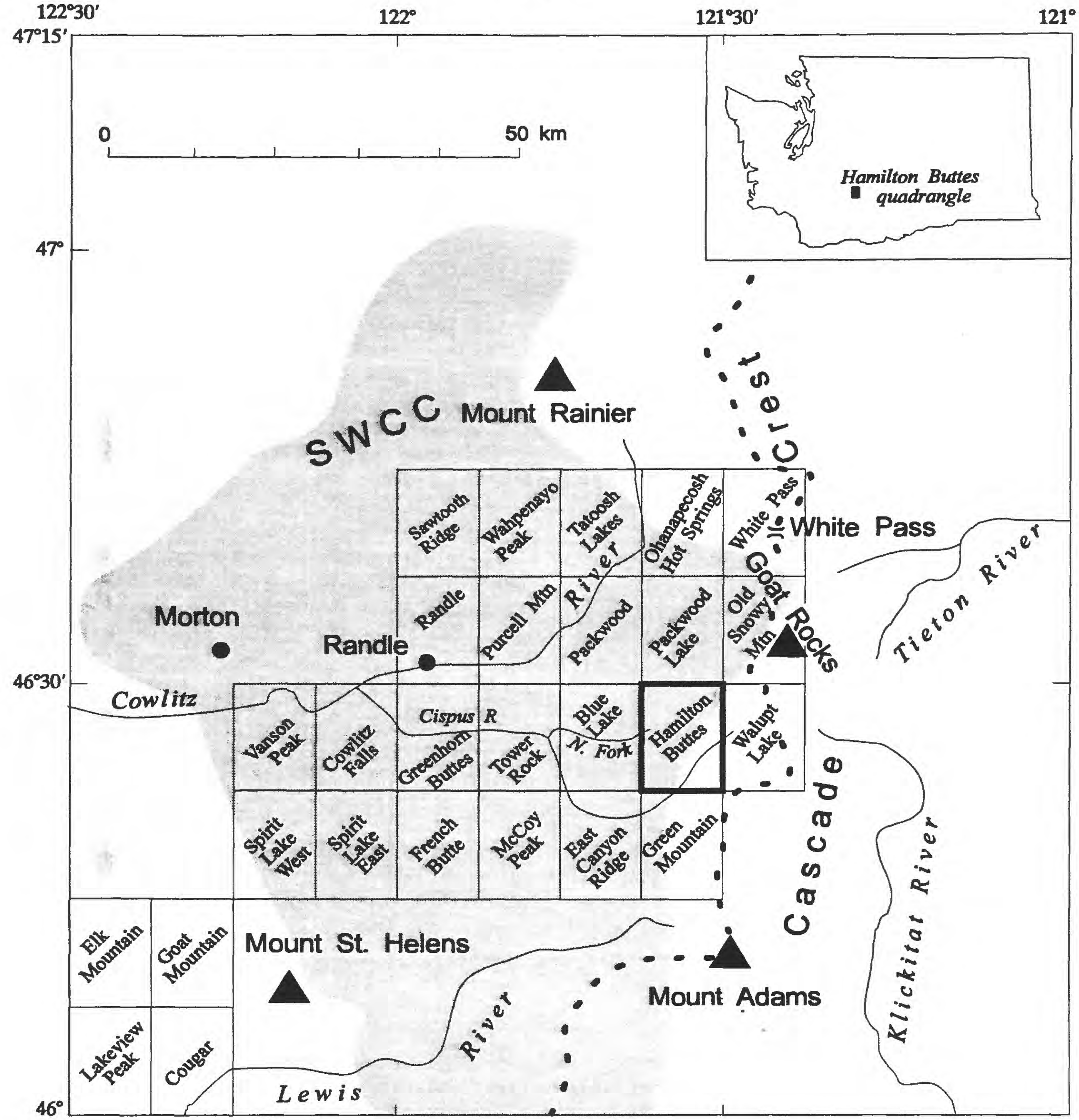


Figure 1. Index map showing location of Hamilton Buttes quadrangle relative to the three Holocene and late Pleistocene composite volcanoes in southern Washington, crest of Cascade Range, Pleistocene–Pliocene volcano at Goat Rocks, Southern Washington Cascades Conductor (SWCC: see text), and other 7-1/2′ quadrangles in which geologic mapping has been completed recently or is planned for the near future. Mapping west of longitude 122° by Russ Evarts and Roger Ashley; mapping east of 122° and south of Cowlitz River by me; mapping north of Cowlitz River by R.B. Moore, C.R. Thornber, and N.G. Banks.

## ACKNOWLEDGMENTS

Paul Hammond and Cynthia Stine introduced me to the Hamilton Buttes area in 1985 and in so doing helped to whet my appetite for the research of the next decade. Mike Korosec kindly provided field maps and chemical analyses that he used to prepare his regional geologic map (Korosec, 1987). Cindy Stine and Warren Winters provided corrected or additional locations for chemical analyses in their theses (Stine, 1987; Winters, 1984). Bob Schuster (U.S. Geological Survey) and Pat Pringle (Washington Division of Geology and Earth Resources) helped me interpret two of the landslides in the area and provided general advice. Barbara White (my wife) provided logistic help on several long traverses. Three programs within the U.S. Geological Survey supported the research—National Cooperative Geologic Mapping (the principal sponsor), National Earthquake Hazards Reduction, and Deep Continental Studies. N.G. Banks reviewed and improved the map and text.

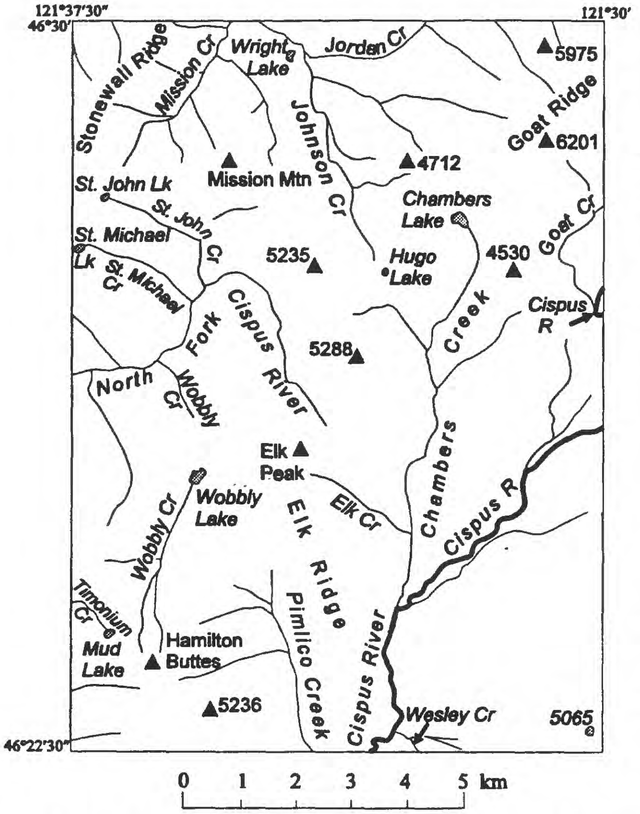


Figure 2. Map of Hamilton Buttes quadrangle showing locations of geographic features mentioned in text.

## ROCK TERMINOLOGY AND CHEMICAL CLASSIFICATION

For consistency, this section follows closely the format of comparable sections in previous open-file reports, including all of the figures. This consistency enables ready comparison with data in the other reports.

I followed the same classification scheme used in previous open-file reports—the IUGS system (Le Bas and others, 1986) modified to include a field for rhyodacite (fig. 3). For the total alkali contents found, the chemically analyzed rocks are grouped under six names: *basalt* (<52 per cent $SiO_2$), *basaltic andesite* (52–57 per cent $SiO_2$), *andesite* (57–63 per cent $SiO_2$), *dacite* (63–68 per cent $SiO_2$), *rhyodacite* (generally between 68 and about 72 percent $SiO_2$; fig. 3), and *rhyolite* (generally greater than about 72 percent $SiO_2$; fig. 3). These samples have rather consistent phenocryst assemblages (fig. 4) (minerals listed in most common order of decreasing abundance): *basalt*, ol ± pl ± cpx ± rare opx; *basaltic andesite*, pl ± cpx ± opx± ol; *andesite*, pl ± cpx ± opx ± rare ol ± hb; *dacite*, assemblage similar to that for andesite (except for rare quartz and no olivine), but orthopyroxene is less common, and the groundmass commonly displays snowflake texture owing to high-temperature devitrification; *rhyodacite* and *rhyolite*, generally almost aphyric with pl > cpx and no quartz. Hornblende occurs only in the intrusive suite of Kidd Creek, the composition of which is silicic andesite and dacite (Marso and Swanson, 1992).

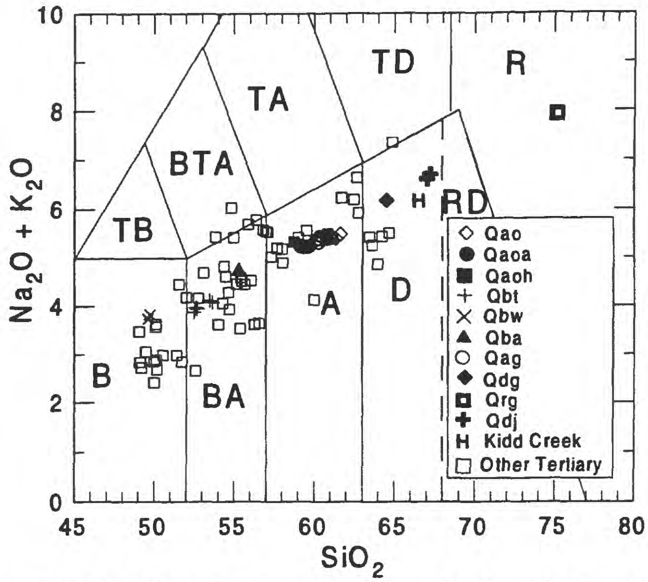


Figure 3. Total alkali-silica classification diagram for chemical analyses of rocks from the Hamilton Buttes quadrangle, modified from Le Bas and others (1986) to include field for rhyodacite. B, basalt; BA, basaltic andesite; A, andesite; D, dacite; RD, rhyodacite; R, rhyolite; TB, trachybasalt; BTA, basaltic trachyandesite; TA, trachyandesite; TD, trachydacite. Data from table 1. Analyses plotted in this and subsequent figures have been normalized to 100 percent on a volatile-free basis, with all iron as FeO* (right half of table 1). Analysis 92 not plotted, because of obvious alkali leaching. Qao, andesite of Old Snowy Mountain; Qaoa, aphyric andesite of Old Snowy Mountain; Qaoh, hornblende andesite of Old Snowy Mountain; Qbt, basalt of Two Lakes; Qbw, basalt of Walupt Lake volcano; Qba, basaltic andesite; Qag, andesite of Goat Ridge; Qdg, dacite of Goat Ridge; Qrg, rhyolite of Goat Ridge; Qdj, dacite of Jordan Creek; Kidd Creek, intrusive suite of Kidd Creek; other Tertiary, Tertiary rocks except intrusive suite of Kidd Creek.

Analysis number 92 (table 1; $Na_2O + K_2O = 2.91$; $SiO_2 = 74.19$) is from a hydrated ash-flow tuff that probably lost both $Na_2O$ and $K_2O$ during alteration. Analysis 79 is from an altered andesite with sericite partly replacing plagioclase; the high $K_2O$ (2.88 percent) and low $Na_2O$ (3.32 percent) may reflect potassic replacement of sodium in the plagioclase. In general the wide scatter in amounts of total alkalies at high silica contents may reflect gains or losses during hydration or other alteration processes. The high $K_2O$ content (4.22 percent) of analysis 93 is apparently real (the rock is fresh, as indicated both in thin section and by the low LOI of the analysis) and indicates a high-K Quaternary rhyolite.

Samples with thin sections but no chemical analyses can be roughly classified by their phenocryst assemblages and groundmass textures (fig. 4). In all, 91 samples from the Hamilton Buttes quadrangle were sectioned (fig. 5); of these, 67 samples were chemically analyzed (table 1). In addition, table 1 includes two chemical analyses previously published by Korosec (1987), seventeen from Winters (1983), and six from Stine (1987). These additional analyses were done in the XRF laboratory of the Geology Department at Washington State University.

The Tertiary suite is barely calcic (Peacock, 1931). Its alkali-lime index is about 61.1 (fig. 6), just on the calcic side of the 61 value separating the calc-alkalic and calcic suites.

## Table 1. Chemical analyses from the Hamilton Buttes quadrangle, arranged in order of increasing $SiO_2$

| Map No. | Map Unit | Field No. | Original Analysis $SiO_2$ | $TiO_2$ | $Al_2O_3$ | $Fe_2O_3$ | FeO | MnO | MgO | CaO | $Na_2O$ | $K_2O$ | $P_2O_5$ | $H_2O^+$ | $H_2O^-$ | $CO_2$ | Total | Recalculated $H_2O$- and $CO_2$-free to 100 percent, with iron as FeO $SiO_2$ | $TiO_2$ | $Al_2O_3$ | FeO* | MnO | MgO | CaO | $Na_2O$ | $K_2O$ | $P_2O_5$ | $Na_2O + K_2O$ | FeO*/ MgO | Longitude Deg | Longitude Min | Latitude Deg | Latitude Min |
|---|---|---|---|---|---|---|---|---|---|---|---|---|---|---|---|---|---|---|---|---|---|---|---|---|---|---|---|---|---|---|---|---|---|
| 1 | Taih | KTT8[1] | 48.9 | 0.74 | 23.5 | 3.77 | 4.32 | 0.13 | 3.98 | 11.17 | 3.26 | 0.21 | 0.08 | | | | 100.01 | 49.05 | 0.74 | 23.57 | 7.74 | 0.13 | 3.99 | 11.21 | 3.27 | 0.21 | 0.08 | 3.48 | 1.94 | 121 | 33.45 | 46 | 25.78 |
| 2 | Tai | 93-066 | 47.1 | 0.75 | 24.0 | 7.11 | | 0.20 | 2.19 | 12.40 | 2.57 | 0.14 | 0.12 | 3.18[7] | | | 99.76 | 49.13 | 0.78 | 25.03 | 6.67 | 0.21 | 2.28 | 12.93 | 2.68 | 0.15 | 0.13 | 2.83 | 2.92 | 121 | 36.60 | 46 | 29.90 |
| 3 | Tg | 93-005 | 47.7 | 0.97 | 20.4 | 9.71 | | 0.16 | 4.54 | 11.60 | 2.36 | 0.28 | 0.15 | 2.17[7] | | | 100.04 | 49.23 | 1.00 | 21.05 | 9.02 | 0.17 | 4.69 | 11.97 | 2.44 | 0.29 | 0.15 | 2.72 | 1.92 | 121 | 36.16 | 46 | 25.98 |
| 4 | Taih | EMM109[1] | 49.3 | 1.12 | 22.7 | 4.43 | 5.08 | 0.19 | 3.42 | 10.67 | 2.99 | 0.05 | 0.13 | | | | 100.00 | 49.48 | 1.12 | 22.76 | 9.11 | 0.19 | 3.44 | 10.72 | 3.00 | 0.05 | 0.13 | 3.05 | 2.65 | 121 | 34.09 | 46 | 27.29 |
| 5 | Qbw | 93-091[3] | 49.3 | 1.53 | 17.3 | 10.60 | | 0.17 | 7.09 | 10.40 | 3.06 | 0.66 | 0.30 | 0.01[7] | | | 100.42 | 49.62 | 1.54 | 17.41 | 9.60 | 0.17 | 7.14 | 10.47 | 3.08 | 0.66 | 0.30 | 3.74 | 1.35 | 121 | 29.56 | 46 | 24.13 |
| 6 | Qbw | 93-096[3] | 49.6 | 1.53 | 17.2 | 10.50 | | 0.17 | 7.31 | 10.30 | 3.06 | 0.76 | 0.35 | 0.01[7] | | | 100.79 | 49.73 | 1.53 | 17.25 | 9.48 | 0.17 | 7.33 | 10.33 | 3.07 | 0.76 | 0.35 | 3.83 | 1.29 | 121 | 28.60 | 46 | 25.30 |
| 7 | Taih | JC400Z[1] | 49.8 | 0.85 | 22.6 | 3.84 | 4.40 | 0.13 | 3.80 | 11.63 | 2.79 | 0.04 | 0.09 | | | | 99.99 | 49.98 | 0.85 | 22.73 | 7.89 | 0.13 | 3.82 | 11.68 | 2.80 | 0.04 | 0.09 | 2.84 | 2.07 | 121 | 33.00 | 46 | 25.15 |
| 8 | Tg | MK98429 | 49.8 | 0.76 | 20.5 | 4.45 | 5.10 | 0.15 | 5.78 | 10.99 | 2.40 | 0.00 | 0.11 | | | | 100.00 | 50.02 | 0.76 | 20.55 | 9.15 | 0.15 | 5.81 | 11.04 | 2.41 | 0.00 | 0.11 | 2.41 | 1.58 | 121 | 36.51 | 46 | 26.30 |
| 9 | Taih | 93-003 | 47.5 | 1.12 | 19.4 | 10.10 | | 0.17 | 4.50 | 9.45 | 2.94 | 0.44 | 0.16 | 4.10[7] | | | 99.88 | 50.12 | 1.18 | 20.47 | 9.59 | 0.18 | 4.75 | 9.97 | 3.10 | 0.46 | 0.17 | 3.57 | 2.02 | 121 | 34.91 | 46 | 27.88 |
| 10 | Taih | MMR104[1] | 49.9 | 1.25 | 19.7 | 5.04 | 5.77 | 0.18 | 4.34 | 10.82 | 2.82 | 0.05 | 0.15 | | | | 100.01 | 50.13 | 1.26 | 19.81 | 10.36 | 0.18 | 4.36 | 10.87 | 2.83 | 0.05 | 0.15 | 2.88 | 2.37 | 121 | 34.62 | 46 | 29.08 |
| 11 | Taih | 93-073 | 48.4 | 1.41 | 19.4 | 10.40 | | 0.16 | 3.54 | 10.60 | 3.23 | 0.27 | 0.17 | 2.46[7] | | | 100.04 | 50.13 | 1.46 | 20.10 | 9.70 | 0.17 | 3.67 | 10.98 | 3.35 | 0.28 | 0.18 | 3.63 | 2.64 | 121 | 34.39 | 46 | 27.07 |
| 12 | Tg | WW-2[2] | 49.6 | 1.13 | 20.4 | 10.12 | | 0.18 | 4.09 | 11.64 | 2.30 | 0.35 | 0.12 | | | | 99.90 | 50.18 | 1.14 | 20.58 | 9.21 | 0.18 | 4.14 | 11.77 | 2.33 | 0.35 | 0.12 | 2.68 | 2.23 | 121 | 36.51 | 46 | 26.30 |
| 13 | (Taih) | EMM114[1] | 50.3 | 1.21 | 19.5 | 5.56 | 6.37 | 0.20 | 4.06 | 9.78 | 2.91 | 0.05 | 0.14 | | | | 100.02 | 50.54 | 1.22 | 19.57 | 11.44 | 0.20 | 4.08 | 9.83 | 2.93 | 0.05 | 0.14 | 2.98 | 2.80 | 121 | 34.10 | 46 | 26.76 |
| 14 | Taih | JC203[1] | 51.2 | 1.48 | 17.6 | 4.33 | 4.96 | 0.22 | 6.69 | 10.34 | 2.95 | 0.02 | 0.22 | | | | 100.00 | 51.40 | 1.49 | 17.69 | 8.90 | 0.22 | 6.72 | 10.38 | 2.96 | 0.02 | 0.22 | 2.98 | 1.32 | 121 | 33.46 | 46 | 27.88 |
| 15 | Taih | KTR309[1] | 51.3 | 1.54 | 18.1 | 4.81 | 5.51 | 0.17 | 5.12 | 8.80 | 3.54 | 0.89 | 0.22 | | | | 100.01 | 51.55 | 1.55 | 18.19 | 9.89 | 0.17 | 5.14 | 8.84 | 3.56 | 0.89 | 0.22 | 4.45 | 1.92 | 121 | 33.16 | 46 | 25.60 |
| 16 | Tai | HG130[1] | 51.4 | 1.86 | 15.7 | 6.21 | 7.12 | 0.25 | 4.61 | 9.80 | 2.77 | 0.05 | 0.20 | | | | 100.00 | 51.72 | 1.87 | 15.83 | 12.79 | 0.25 | 4.64 | 9.86 | 2.79 | 0.05 | 0.20 | 2.84 | 2.76 | 121 | 33.10 | 46 | 28.67 |
| 17 | Taih | GR82-098 | 50.4 | 1.60 | 19.5 | 4.79 | 4.00 | 0.17 | 3.22 | 9.35 | 3.10 | 0.95 | 0.32 | 1.64 | 0.49 | 0.00 | 99.53 | 52.00 | 1.65 | 20.12 | 8.58 | 0.18 | 3.32 | 9.65 | 3.20 | 0.98 | 0.33 | 4.18 | 2.58 | 121 | 30.87 | 46 | 29.80 |
| 18 | Qbt | 93-018 | 51.9 | 1.23 | 17.1 | 9.66 | | 0.15 | 6.58 | 9.18 | 3.14 | 0.70 | 0.18 | 0.16[7] | | | 99.98 | 52.50 | 1.24 | 17.30 | 8.79 | 0.15 | 6.66 | 9.29 | 3.18 | 0.71 | 0.18 | 3.88 | 1.32 | 121 | 31.05 | 46 | 24.47 |
| 19 | Qbt | 93-020 | 52.3 | 1.26 | 17.1 | 9.82 | | 0.15 | 6.56 | 9.06 | 3.26 | 0.69 | 0.18 | 0.01[7] | | | 100.39 | 52.62 | 1.27 | 17.20 | 8.89 | 0.15 | 6.60 | 9.11 | 3.28 | 0.69 | 0.18 | 3.97 | 1.35 | 121 | 32.08 | 46 | 23.50 |
| 20 | Ta | 93-006 | 48.1 | 1.79 | 14.6 | 12.90 | | 0.20 | 3.93 | 8.49 | 2.31 | 0.12 | 0.25 | 7.45[7] | | | 92.69 | 52.63 | 1.96 | 15.97 | 12.70 | 0.22 | 4.30 | 9.29 | 2.53 | 0.13 | 0.27 | 2.66 | 2.95 | 121 | 32.90 | 46 | 26.94 |
| 21 | Qbt | 93-019 | 52.4 | 1.23 | 17.1 | 9.76 | | 0.15 | 6.59 | 9.09 | 3.24 | 0.69 | 0.18 | 0.01[7] | | | 100.44 | 52.69 | 1.24 | 17.19 | 8.83 | 0.15 | 6.63 | 9.14 | 3.26 | 0.69 | 0.18 | 3.95 | 1.33 | 121 | 31.10 | 46 | 24.45 |
| 22 | Taih | 92-108 | 50.6 | 1.20 | 19.1 | 8.95 | | 0.14 | 2.99 | 9.61 | 3.21 | 0.79 | 0.21 | 2.94[7] | | | 99.74 | 52.76 | 1.25 | 19.92 | 8.40 | 0.15 | 3.12 | 10.02 | 3.35 | 0.82 | 0.22 | 4.17 | 2.69 | 121 | 0.93 | 46 | 25.94 |
| 23 | Taih | KTR404[1] | 52.9 | 1.35 | 19.7 | 4.45 | 5.10 | 0.15 | 3.11 | 8.42 | 3.66 | 1.01 | 0.20 | | | | 99.99 | 53.11 | 1.36 | 19.76 | 9.15 | 0.15 | 3.12 | 8.46 | 3.68 | 1.01 | 0.20 | 4.69 | 2.93 | 121 | 32.95 | 46 | 25.94 |
| 24 | Qbt | 93-035 | 52.9 | 1.21 | 17.2 | 9.41 | | 0.15 | 5.92 | 8.84 | 3.19 | 0.89 | 0.21 | 0.14[7] | | | 100.06 | 53.45 | 1.22 | 17.38 | 8.56 | 0.15 | 5.98 | 8.93 | 3.22 | 0.90 | 0.21 | 4.12 | 1.43 | 121 | 30.19 | 46 | 23.18 |
| 25 | Qbt | 93-072 | 53.4 | 1.14 | 16.9 | 9.38 | | 0.15 | 6.82 | 8.48 | 3.13 | 0.93 | 0.20 | 0.15[7] | | | 100.68 | 53.62 | 1.14 | 16.97 | 8.48 | 0.15 | 6.85 | 8.51 | 3.14 | 0.93 | 0.20 | 4.08 | 1.24 | 121 | 31.73 | 46 | 23.77 |
| 26 | Tai | 93-022 | 51.8 | 1.95 | 15.5 | 13.40 | | 0.22 | 2.91 | 6.35 | 4.55 | 0.67 | 0.21 | 2.49[7] | | | 100.05 | 53.83 | 2.03 | 16.11 | 12.53 | 0.23 | 3.02 | 6.60 | 4.73 | 0.70 | 0.22 | 5.43 | 4.14 | 121 | 32.80 | 46 | 27.77 |
| 27 | Tai | EEW-9[2] | 53.4 | 1.64 | 17.8 | 10.52 | | 0.15 | 3.34 | 9.15 | 2.47 | 1.12 | 0.26 | | | | 99.87 | 54.03 | 1.66 | 18.04 | 9.58 | 0.15 | 3.38 | 9.26 | 2.50 | 1.13 | 0.26 | 3.63 | 2.83 | 121 | 35.33 | 46 | 24.80 |
| 28 | Tai | 91-076 | 53.2 | 1.29 | 18.5 | 2.81 | 5.29 | 0.14 | 3.67 | 9.24 | 3.36 | 0.62 | 0.19 | 0.92 | 0.72 | 0.00 | 99.95 | 54.27 | 1.32 | 18.87 | 7.98 | 0.14 | 3.74 | 9.43 | 3.43 | 0.63 | 0.19 | 4.06 | 2.13 | 121 | 37.37 | 46 | 24.45 |
| 29 | Tai | HB-26[2] | 53.8 | 1.37 | 18.7 | 9.28 | | 0.14 | 3.71 | 7.98 | 3.87 | 0.91 | 0.16 | | | | 99.87 | 54.38 | 1.38 | 18.85 | 8.44 | 0.14 | 3.75 | 8.07 | 3.91 | 0.92 | 0.16 | 4.83 | 2.25 | 121 | 36.98 | 46 | 24.05 |
| 30 | Tai | 91-075 | 53.0 | 1.17 | 17.9 | 2.82 | 5.49 | 0.14 | 3.91 | 8.46 | 3.87 | 0.62 | 0.20 | 1.44 | 0.91 | 0.00 | 99.93 | 54.47 | 1.20 | 18.40 | 8.25 | 0.14 | 4.02 | 8.69 | 3.98 | 0.64 | 0.21 | 4.61 | 2.05 | 121 | 37.45 | 46 | 24.26 |
| 31 | Tai | EW-7[2] | 54.0 | 1.46 | 17.7 | 10.57 | | 0.21 | 3.68 | 7.76 | 3.50 | 0.74 | 0.25 | | | | 99.88 | 54.65 | 1.48 | 17.91 | 9.63 | 0.21 | 3.72 | 7.85 | 3.54 | 0.75 | 0.25 | 4.29 | 2.59 | 121 | 35.78 | 46 | 24.40 |
| 32 | Tai | EEW-7` | 54.1 | 1.44 | 17.5 | 10.06 | | 0.22 | 4.18 | 8.34 | 3.23 | 0.66 | 0.21 | | | | 99.84 | 54.69 | 1.46 | 17.66 | 9.16 | 0.22 | 4.23 | 8.44 | 3.27 | 0.67 | 0.21 | 3.94 | 2.17 | 121 | 35.23 | 46 | 24.74 |
| 33 | Tai | 93-069 | 50.9 | 1.83 | 15.3 | 11.30 | | 0.16 | 3.31 | 5.04 | 4.46 | 1.14 | 0.54 | 5.64[7] | | | 99.62 | 54.82 | 1.97 | 16.48 | 10.95 | 0.17 | 3.56 | 5.43 | 4.80 | 1.23 | 0.58 | 6.03 | 3.07 | 121 | 33.47 | 46 | 29.63 |
| 34 | Taih | 93-016 | 52.1 | 1.79 | 15.8 | 10.60 | | 0.16 | 3.13 | 6.74 | 4.20 | 0.94 | 0.36 | 3.49[7] | | | 99.31 | 54.98 | 1.89 | 16.67 | 10.07 | 0.17 | 3.30 | 7.11 | 4.43 | 0.99 | 0.38 | 5.42 | 3.05 | 121 | 33.05 | 46 | 27.48 |
| 35 | Taih | HG100[1] | 54.9 | 1.83 | 17.3 | 4.67 | 5.35 | 0.16 | 3.29 | 7.74 | 3.57 | 0.87 | 0.33 | | | | 100.00 | 55.16 | 1.84 | 17.37 | 9.60 | 0.16 | 3.31 | 7.78 | 3.59 | 0.87 | 0.33 | 4.46 | 2.90 | 121 | 33.05 | 46 | 27.48 |
| 36 | Qba | 93-071 | 54.5 | 1.29 | 16.8 | 8.30 | | 0.13 | 4.83 | 8.55 | 3.32 | 1.38 | 0.29 | 0.58[7] | | | 99.97 | 55.30 | 1.31 | 17.05 | 7.58 | 0.13 | 4.90 | 8.67 | 3.37 | 1.40 | 0.29 | 4.77 | 1.55 | 121 | 31.30 | 46 | 24.43 |
| 37 | Tai | NR-14[2,4] | 54.8 | 1.55 | 17.9 | 10.01 | | 0.16 | 2.85 | 8.89 | 2.67 | 0.83 | 0.26 | | | | 99.89 | 55.43 | 1.57 | 18.06 | 9.11 | 0.16 | 2.88 | 8.99 | 2.70 | 0.84 | 0.26 | 3.54 | 3.16 | 121 | 37.48 | 46 | 26.53 |
| 38 | Tai | 93-057 | 54.4 | 1.24 | 16.8 | 8.70 | | 0.14 | 5.12 | 7.88 | 3.61 | 0.89 | 0.23 | 1.06[7] | | | 100.07 | 55.43 | 1.26 | 17.12 | 7.98 | 0.14 | 5.22 | 8.03 | 3.68 | 0.91 | 0.23 | 4.59 | 1.53 | 121 | 35.96 | 46 | 23.49 |
| 39 | Tdip | 92-102 | 53.8 | 1.23 | 17.0 | 8.78 | | 0.14 | 4.10 | 8.16 | 3.47 | 0.91 | 0.24 | 1.84[7] | | | 99.67 | 55.49 | 1.27 | 17.53 | 8.15 | 0.14 | 4.23 | 8.42 | 3.58 | 0.94 | 0.25 | 4.52 | 1.93 | 121 | 34.21 | 46 | 22.84 |
| 40 | Tai | 93-059 | 54.5 | 1.25 | 16.6 | 8.69 | | 0.14 | 5.03 | 7.98 | 3.46 | 0.90 | 0.23 | 0.91[7] | | | 99.69 | 55.66 | 1.28 | 16.95 | 7.99 | 0.14 | 5.14 | 8.15 | 3.53 | 0.92 | 0.23 | 4.45 | 1.55 | 121 | 36.60 | 46 | 23.46 |
| 41 | Tai | 93-027 | 54.1 | 1.27 | 17.4 | 8.46 | | 0.24 | 4.06 | 6.34 | 4.25 | 1.26 | 0.24 | 2.24[7] | | | 99.86 | 55.90 | 1.31 | 17.98 | 7.87 | 0.25 | 4.20 | 6.55 | 4.39 | 1.30 | 0.25 | 5.69 | 1.88 | 121 | 35.42 | 46 | 23.65 |
| 42 | Tg | EMM147[1] | 55.8 | 1.25 | 17.3 | 4.04 | 4.63 | 0.14 | 4.05 | 8.05 | 3.63 | 0.88 | 0.21 | | | | 100.00 | 56.06 | 1.26 | 17.36 | 8.30 | 0.14 | 4.07 | 8.08 | 3.64 | 0.88 | 0.21 | 4.53 | 2.04 | 121 | 35.44 | 46 | 27.29 |
| 43 | Tai | 93-058 | 55.0 | 1.23 | 16.1 | 8.94 | | 0.15 | 4.85 | 8.56 | 2.96 | 0.58 | 0.24 | 1.63[7] | | | 100.24 | 56.29 | 1.26 | 16.48 | 8.23 | 0.15 | 4.96 | 8.76 | 3.03 | 0.59 | 0.25 | 3.62 | 1.66 | 121 | 36.02 | 46 | 23.49 |
| 44 | Tai | MCR191[1] | 56.1 | 1.51 | 16.7 | 4.95 | 5.67 | 0.20 | 2.82 | 5.95 | 4.19 | 1.56 | 0.38 | | | | 100.01 | 56.39 | 1.52 | 16.74 | 10.17 | 0.20 | 2.83 | 5.98 | 4.21 | 1.57 | 0.38 | 5.78 | 3.59 | 121 | 35.12 | 46 | 29.82 |
| 45 | Tai | MK98426 | 56.4 | 1.20 | 15.7 | 4.26 | 4.88 | 0.15 | 5.01 | 8.63 | 3.17 | 0.46 | 0.21 | | | | 100.00 | 56.59 | 1.21 | 15.75 | 8.75 | 0.15 | 5.03 | 8.67 | 3.18 | 0.46 | 0.21 | 3.65 | 1.74 | 121 | 36.25 | 46 | 23.46 |
| 46 | Tai | 92-107 | 54.5 | 1.55 | 15.3 | 11.30 | | 0.20 | 3.03 | 5.50 | 4.54 | 0.81 | 0.31 | 2.63[7] | | | 99.67 | 56.82 | 1.62 | 15.95 | 10.60 | 0.21 | 3.16 | 5.73 | 4.73 | 0.84 | 0.32 | 5.58 | 3.36 | 121 | 32.90 | 46 | 26.00 |
| 47 | Tai | 93-054 | 55.1 | 1.49 | 15.4 | 11.00 | | 0.21 | 2.83 | 5.99 | 4.04 | 1.32 | 0.39 | 2.11[7] | | | 99.88 | 57.00 | 1.54 | 15.93 | 10.24 | 0.22 | 2.93 | 6.20 | 4.18 | 1.37 | 0.40 | 5.54 | 3.50 | 121 | 35.12 | 46 | 29.82 |
| 48 | Taih | 91-024 | 55.7 | 1.15 | 16.2 | 3.67 | 4.95 | 0.15 | 3.79 | 6.69 | 3.99 | 1.40 | 0.23 | 1.68 | 0.30 | 0.00 | 99.90 | 57.10 | 1.18 | 16.61 | 8.46 | 0.15 | 3.89 | 6.86 | 4.09 | 1.44 | 0.24 | 5.53 | 2.18 | 121 | 35.76 | 46 | 27.67 |
| 49 | Tai | 93-078 | 53.8 | 1.26 | 16.4 | 7.94 | | 0.14 | 2.99 | 7.07 | 3.33 | 1.38 | 0.38 | 5.09[7] | | | 99.78 | 57.30 | 1.34 | 17.47 | 7.61 | 0.15 | 3.18 | 7.53 | 3.55 | 1.47 | 0.40 | 5.02 | 2.39 | 121 | 30.98 | 46 | 29.81 |
| 50 | Tai | 91-026 | 56.0 | 1.54 | 16.2 | 3.54 | 5.39 | 0.15 | 2.92 | 6.38 | 3.61 | 1.44 | 0.29 | 1.73 | 0.64 | 0.03 | 99.86 | 57.67 | 1.59 | 16.68 | 8.83 | 0.15 | 3.01 | 6.57 | 3.72 | 1.48 | 0.30 | 5.20 | 2.94 | 121 | 36.93 | 46 | 26.28 |
| 51 | Tai | 93-077 | 55.6 | 1.14 | 16.7 | 7.53 | | 0.14 | 3.22 | 7.01 | 3.42 | 1.55 | 0.32 | 3.13[7] | | | 99.76 | 57.99 | 1.19 | 17.42 | 7.07 | 0.15 | 3.36 | 7.31 | 3.57 | 1.62 | 0.33 | 5.18 | 2.10 | 121 | 31.09 | 46 | 29.88 |
| 52 | Tai | 93-053 | 56.0 | 1.56 | 15.7 | 8.55 | | 0.15 | 3.27 | 6.95 | 3.51 | 1.21 | 0.44 | 2.76[7] | | | 100.10 | 58.04 | 1.62 | 16.27 | 7.98 | 0.16 | 3.39 | 7.20 | 3.64 | 1.25 | 0.46 | 4.89 | 2.35 | 121 | 37.05 | 46 | 28.18 |
| 53 | Qaoh | 93-042[3] | 58.2 | 1.07 | 17.4 | 7.08 | | 0.11 | 3.62 | 6.71 | 3.89 | 1.39 | 0.34 | 0.08[7] | | | 99.89 | 58.73 | 1.08 | 17.56 | 6.43 | 0.11 | 3.65 | 6.77 | 3.93 | 1.40 | 0.34 | 5.33 | 1.76 | 121 | 29.99 | 46 | 27.17 |
| 54 | Tai | 91-022 | 55.7 | 1.17 | 16.2 | 3.29 | 4.30 | 0.13 | 2.39 | 6.14 | 3.64 | 1.48 | 0.29 | 0.85 | 1.04 | 0.00 | 96.62 | 59.00 | 1.24 | 17.16 | 7.69 | 0.14 | 2.53 | 6.50 | 3.86 | 1.57 | 0.31 | 5.42 | 3.04 | 121 | 36.36 | 46 | 26.73 |

Table 1. Chemical analyses from the Hamilton Buttes quadrangle, arranged in order of increasing $SiO_2$ (cont.)

| Map No. | Map Unit | Field No. | Original Analysis $SiO_2$ | $TiO_2$ | $Al_2O_3$ | $Fe_2O_3$ | FeO | MnO | MgO | CaO | $Na_2O$ | $K_2O$ | $P_2O_5$ | $H_2O^+$ | $H_2O^-$ | $CO_2$ | Total | Recalculated $H_2O$- and $CO_2$-free to 100 percent, with iron as FeO $SiO_2$ | $TiO_2$ | $Al_2O_3$ | FeO* | MnO | MgO | CaO | $Na_2O$ | $K_2O$ | $P_2O_5$ | $Na_2O + K_2O$ | FeO*/ MgO | Longitude Deg | Longitude Min | Latitude Deg | Latitude Min |
|---|---|---|---|---|---|---|---|---|---|---|---|---|---|---|---|---|---|---|---|---|---|---|---|---|---|---|---|---|---|---|---|---|---|
| 55 | Qaoa | 93-037 | 58.6 | 1.06 | 17.3 | 7.07 | | 0.11 | 3.54 | 6.57 | 3.81 | 1.38 | 0.34 | 0.01[7] | | | 99.79 | 59.15 | 1.07 | 17.46 | 6.42 | 0.11 | 3.57 | 6.63 | 3.85 | 1.39 | 0.34 | 5.24 | 1.80 | 121 | 30.18 | 46 | 25.76 |
| 56 | Qag? | 93-013 | 58.7 | 1.05 | 17.4 | 7.00 | | 0.11 | 3.43 | 6.46 | 3.79 | 1.35 | 0.33 | 0.35[7] | | | 99.97 | 59.34 | 1.06 | 17.59 | 6.37 | 0.11 | 3.47 | 6.53 | 3.83 | 1.36 | 0.33 | 5.20 | 1.84 | 121 | 30.65 | 46 | 27.31 |
| 57 | Tai | 93-033 | 56.3 | 1.00 | 17.4 | 6.43 | | 0.09 | 2.86 | 5.58 | 4.45 | 0.81 | 0.29 | 4.28[7] | | | 99.49 | 59.53 | 1.06 | 18.40 | 6.12 | 0.10 | 3.02 | 5.90 | 4.71 | 0.86 | 0.31 | 5.56 | 2.02 | 121 | 36.78 | 46 | 22.52 |
| 58 | Qaoa | 93-017 | 59.2 | 1.04 | 17.3 | 7.07 | | 0.11 | 3.34 | 6.49 | 3.80 | 1.39 | 0.32 | 0.01[7] | | | 100.07 | 59.59 | 1.05 | 17.41 | 6.40 | 0.11 | 3.36 | 6.53 | 3.82 | 1.40 | 0.32 | 5.22 | 1.91 | 121 | 30.45 | 46 | 24.86 |
| 59 | Qaoa | 93-038 | 58.9 | 1.03 | 17.2 | 7.01 | | 0.11 | 3.35 | 6.38 | 3.79 | 1.38 | 0.31 | 0.01[7] | | | 99.47 | 59.64 | 1.04 | 17.42 | 6.39 | 0.11 | 3.39 | 6.46 | 3.84 | 1.40 | 0.31 | 5.23 | 1.88 | 121 | 30.14 | 46 | 25.82 |
| 61[8] | Ta | 93-079 | 58.1 | 1.10 | 15.9 | 7.43 | | 0.12 | 3.28 | 7.40 | 2.53 | 1.46 | 0.29 | 1.94[7] | | | 99.55 | 59.98 | 1.14 | 16.41 | 6.90 | 0.12 | 3.39 | 7.64 | 2.61 | 1.51 | 0.30 | 4.12 | 2.04 | 121 | 30.12 | 46 | 29.55 |
| 62 | Qag | 93-045 | 59.3 | 1.02 | 17.0 | 6.95 | | 0.10 | 3.23 | 6.20 | 3.79 | 1.49 | 0.35 | 0.01[7] | | | 99.44 | 60.06 | 1.03 | 17.22 | 6.34 | 0.10 | 3.27 | 6.28 | 3.84 | 1.51 | 0.35 | 5.35 | 1.94 | 121 | 30.84 | 46 | 28.89 |
| 63 | Qag | GR82-066 | 59.4 | 1.02 | 16.9 | 1.94 | 4.52 | 0.11 | 3.18 | 6.23 | 3.71 | 1.52 | 0.32 | 0.11 | 0.28 | 0.00 | 99.24 | 60.21 | 1.03 | 17.13 | 6.35 | 0.11 | 3.22 | 6.31 | 3.76 | 1.54 | 0.32 | 5.30 | 1.97 | 121 | 30.87 | 46 | 29.00 |
| 64 | Qag | 93-081 | 59.8 | 1.04 | 17.0 | 6.99 | | 0.11 | 3.16 | 6.24 | 3.81 | 1.52 | 0.34 | 0.04[7] | | | 100.05 | 60.21 | 1.05 | 17.12 | 6.33 | 0.11 | 3.18 | 6.28 | 3.84 | 1.53 | 0.34 | 5.37 | 1.99 | 121 | 32.68 | 46 | 29.34 |
| 65 | Qag | GR82-082 | 59.6 | 1.02 | 16.8 | 2.58 | 3.93 | 0.11 | 3.31 | 6.20 | 3.76 | 1.48 | 0.31 | 0.28 | 0.13 | 0.00 | 99.51 | 60.30 | 1.03 | 17.00 | 6.33 | 0.11 | 3.35 | 6.27 | 3.80 | 1.50 | 0.31 | 5.30 | 1.89 | 121 | 30.55 | 46 | 28.28 |
| 66 | Qag | HG104[1] | 60.1 | 0.97 | 17.4 | 3.04 | 3.48 | 0.10 | 3.27 | 5.87 | 3.90 | 1.53 | 0.28 | | | | 99.99 | 60.32 | 0.97 | 17.47 | 6.24 | 0.10 | 3.28 | 5.89 | 3.91 | 1.53 | 0.28 | 5.45 | 1.90 | 121 | 31.90 | 46 | 27.20 |
| 67 | Qag | GR82-115 | 59.5 | 1.02 | 16.8 | 2.09 | 4.39 | 0.11 | 3.19 | 6.09 | 3.74 | 1.55 | 0.33 | 0.30 | 0.09 | 0.00 | 99.20 | 60.34 | 1.03 | 17.04 | 6.36 | 0.11 | 3.24 | 6.18 | 3.79 | 1.57 | 0.33 | 5.37 | 1.97 | 121 | 31.03 | 46 | 27.95 |
| 68 | Qag | 93-046 | 59.9 | 1.03 | 16.9 | 6.85 | | 0.11 | 2.97 | 6.21 | 3.85 | 1.53 | 0.35 | 0.01[7] | | | 99.71 | 60.50 | 1.04 | 17.07 | 6.23 | 0.11 | 3.00 | 6.27 | 3.89 | 1.55 | 0.35 | 5.43 | 2.08 | 121 | 31.21 | 46 | 28.52 |
| 69 | Qag | 93-051 | 60.2 | 1.00 | 16.9 | 6.72 | | 0.11 | 3.02 | 6.03 | 3.85 | 1.58 | 0.34 | 0.01[7] | | | 99.76 | 60.76 | 1.01 | 17.06 | 6.10 | 0.11 | 3.05 | 6.09 | 3.89 | 1.59 | 0.34 | 5.48 | 2.00 | 121 | 32.47 | 46 | 28.82 |
| 70 | Qag | 93-010 | 60.3 | 1.01 | 16.9 | 6.85 | | 0.10 | 3.07 | 5.96 | 3.77 | 1.56 | 0.34 | 0.20[7] | | | 100.06 | 60.80 | 1.02 | 17.04 | 6.22 | 0.10 | 3.10 | 6.01 | 3.80 | 1.57 | 0.34 | 5.37 | 2.01 | 121 | 31.85 | 46 | 26.03 |
| 71 | Qaoh | 93-047 | 60.3 | 0.94 | 16.9 | 6.53 | | 0.11 | 3.11 | 6.13 | 3.94 | 1.50 | 0.31 | 0.01[7] | | | 99.78 | 60.84 | 0.95 | 17.05 | 5.93 | 0.11 | 3.14 | 6.18 | 3.98 | 1.51 | 0.31 | 5.49 | 1.89 | 121 | 30.02 | 46 | 28.46 |
| 72 | Qag | 93-085 | 60.5 | 1.00 | 16.8 | 6.81 | | 0.11 | 2.97 | 6.00 | 3.87 | 1.55 | 0.34 | 0.01[7] | | | 99.96 | 60.95 | 1.01 | 16.92 | 6.17 | 0.11 | 2.99 | 6.04 | 3.90 | 1.56 | 0.34 | 5.46 | 2.06 | 121 | 30.39 | 46 | 28.37 |
| 73 | Qag | 93-009 | 60.6 | 0.99 | 16.9 | 6.74 | | 0.10 | 3.02 | 6.02 | 3.81 | 1.55 | 0.33 | 0.01[7] | | | 100.07 | 60.97 | 1.00 | 17.00 | 6.10 | 0.10 | 3.04 | 6.06 | 3.83 | 1.56 | 0.33 | 5.39 | 2.01 | 121 | 32.68 | 46 | 25.22 |
| 74 | Qag | 93-044 | 60.4 | 1.00 | 16.9 | 6.75 | | 0.10 | 2.93 | 5.84 | 3.79 | 1.57 | 0.35 | 0.19[7] | | | 99.82 | 61.04 | 1.01 | 17.08 | 6.14 | 0.10 | 2.96 | 5.90 | 3.83 | 1.59 | 0.35 | 5.42 | 2.07 | 121 | 31.13 | 46 | 28.73 |
| 75 | Qag | 93-014 | 60.6 | 0.99 | 16.8 | 6.80 | | 0.10 | 2.95 | 5.90 | 3.80 | 1.56 | 0.35 | 0.08[7] | | | 99.93 | 61.11 | 1.00 | 16.94 | 6.17 | 0.10 | 2.97 | 5.95 | 3.83 | 1.57 | 0.35 | 5.40 | 2.07 | 121 | 31.31 | 46 | 27.46 |
| 76 | Qao | 93-012 | 60.9 | 0.94 | 16.9 | 6.49 | | 0.10 | 3.07 | 5.86 | 3.85 | 1.51 | 0.32 | 0.11[7] | | | 100.05 | 61.33 | 0.95 | 17.02 | 5.88 | 0.10 | 3.09 | 5.90 | 3.88 | 1.52 | 0.32 | 5.40 | 1.90 | 121 | 30.36 | 46 | 25.75 |
| 77 | Qao | 93-011 | 61.2 | 0.90 | 16.7 | 6.39 | | 0.10 | 3.01 | 5.89 | 3.93 | 1.52 | 0.31 | 0.05[7] | | | 100.00 | 61.62 | 0.91 | 16.82 | 5.79 | 0.10 | 3.03 | 5.93 | 3.96 | 1.53 | 0.31 | 5.49 | 1.91 | 121 | 30.66 | 46 | 26.79 |
| 78 | Tai | 93-055 | 59.8 | 0.94 | 16.9 | 6.95 | | 0.13 | 1.51 | 4.99 | 4.74 | 1.30 | 0.33 | 2.36[7] | | | 99.95 | 61.72 | 0.97 | 17.44 | 6.46 | 0.13 | 1.56 | 5.15 | 4.89 | 1.34 | 0.34 | 6.23 | 4.14 | 121 | 36.58 | 46 | 29.53 |
| 79 | Ta | 93-084 | 59.5 | 0.95 | 15.1 | 5.94 | | 0.11 | 3.00 | 5.12 | 3.16 | 2.74 | 0.25 | 3.91[7] | | | 99.78 | 62.45 | 1.00 | 15.85 | 5.61 | 0.12 | 3.15 | 5.37 | 3.32 | 2.88 | 0.26 | 6.19 | 1.78 | 121 | 30.34 | 46 | 29.09 |
| 80 | Tai | 93-082 | 61.2 | 0.75 | 14.9 | 9.87 | | 0.21 | 0.79 | 4.16 | 5.27 | 1.22 | 0.31 | 1.45[7] | | | 100.13 | 62.65 | 0.77 | 15.25 | 9.09 | 0.21 | 0.81 | 4.26 | 5.39 | 1.25 | 0.32 | 6.64 | 11.24 | 121 | 34.04 | 46 | 28.92 |
| 81 | Tai | 93-062 | 60.7 | 1.07 | 14.8 | 8.99 | | 0.17 | 1.51 | 4.39 | 4.61 | 1.12 | 0.29 | 1.96[7] | | | 99.61 | 62.74 | 1.11 | 15.30 | 8.36 | 0.18 | 1.56 | 4.54 | 4.76 | 1.16 | 0.30 | 5.92 | 5.36 | 121 | 37.08 | 46 | 28.58 |
| 82 | Tai | BT1S[1] | 63.1 | 0.72 | 15.0 | 4.57 | 5.24 | 0.21 | 0.62 | 4.86 | 4.63 | 0.76 | 0.23 | | | | 99.99 | 63.43 | 0.72 | 15.09 | 9.40 | 0.21 | 0.62 | 4.88 | 4.65 | 0.76 | 0.23 | 5.42 | 15.09 | 121 | 34.09 | 46 | 28.86 |
| 83 | Tai | BT10[1] | 63.3 | 0.72 | 15.1 | 4.46 | 5.11 | 0.20 | 0.62 | 4.99 | 3.94 | 1.29 | 0.25 | | | | 100.00 | 63.58 | 0.72 | 15.19 | 9.16 | 0.20 | 0.62 | 5.01 | 3.96 | 1.30 | 0.25 | 5.25 | 14.72 | 121 | 34.08 | 46 | 28.94 |
| 84 | Tai | JOR104[1] | 63.7 | 0.70 | 15.3 | 4.25 | 4.86 | 0.20 | 0.54 | 5.37 | 3.81 | 1.03 | 0.22 | | | | 100.00 | 63.95 | 0.70 | 15.41 | 8.72 | 0.20 | 0.54 | 5.39 | 3.83 | 1.03 | 0.22 | 4.86 | 16.08 | 121 | 33.85 | 46 | 29.64 |
| 85 | Tai | 93-070 | 60.1 | 0.69 | 14.2 | 9.17 | | 0.19 | 0.68 | 4.14 | 4.14 | 0.94 | 0.27 | 5.08[7] | | | 99.60 | 64.21 | 0.74 | 15.17 | 8.82 | 0.20 | 0.73 | 4.42 | 4.42 | 1.00 | 0.29 | 5.43 | 12.14 | 121 | 33.90 | 46 | 29.62 |
| 86 | Qdg | GR82-100 | 63.7 | 0.84 | 16.2 | 1.60 | 3.37 | 0.08 | 2.09 | 4.73 | 3.77 | 2.33 | 0.19 | 0.24 | 0.17 | 0.00 | 99.31 | 64.51 | 0.85 | 16.41 | 4.87 | 0.08 | 2.12 | 4.79 | 3.82 | 2.36 | 0.19 | 6.18 | 2.30 | 121 | 31.75 | 46 | 29.36 |
| 87 | Tai | 93-034 | 61.2 | 0.66 | 16.4 | 4.75 | | 0.08 | 2.34 | 4.29 | 4.06 | 1.15 | 0.20 | 4.44[7] | | | 99.57 | 64.66 | 0.70 | 17.33 | 4.52 | 0.08 | 2.47 | 4.53 | 4.29 | 1.21 | 0.21 | 5.50 | 1.83 | 121 | 37.31 | 46 | 22.65 |
| 88 | Ta | GR82-065 | 62.7 | 0.73 | 16.4 | 5.98 | 0.87 | 0.06 | 0.54 | 2.61 | 4.74 | 2.37 | 0.25 | 1.31 | 0.58 | 0.00 | 99.14 | 64.87 | 0.76 | 16.97 | 6.47 | 0.06 | 0.56 | 2.70 | 4.90 | 2.45 | 0.26 | 7.36 | 11.58 | 121 | 30.90 | 46 | 29.07 |
| 89 | Thd | 92-104[5] | 64.8 | 0.57 | 16.2 | 4.27 | | 0.09 | 1.71 | 4.00 | 4.48 | 1.53 | 0.20 | 1.73[7] | | | 99.58 | 66.51 | 0.59 | 16.63 | 3.94 | 0.09 | 1.76 | 4.11 | 4.60 | 1.57 | 0.21 | 6.17 | 2.25 | 121 | 34.94 | 46 | 22.34 |
| 90 | Qdj | 93-080 | 66.5 | 0.65 | 15.6 | 4.39 | | 0.07 | 1.73 | 3.93 | 3.94 | 2.62 | 0.19 | 0.34[7] | | | 99.96 | 67.05 | 0.66 | 15.73 | 3.98 | 0.07 | 1.74 | 3.96 | 3.97 | 2.64 | 0.19 | 6.61 | 2.28 | 121 | 33.65 | 46 | 29.84 |
| 91 | Qdj | JOR102[1, 6] | 67.1 | 0.66 | 15.9 | 2.03 | 2.33 | 0.07 | 1.53 | 3.56 | 3.87 | 2.82 | 0.14 | | | | 99.99 | 67.25 | 0.66 | 15.90 | 4.17 | 0.07 | 1.53 | 3.57 | 3.88 | 2.83 | 0.14 | 6.70 | 2.72 | 121 | 33.06 | 46 | 30.01 |
| 92 | Ttv | 93-061 | 66.3 | 0.30 | 12.6 | 2.79 | | 0.06 | 0.47 | 4.42 | 1.49 | 1.11 | 0.10 | 10.10[7] | | | 99.74 | 74.19 | 0.34 | 14.10 | 2.81 | 0.07 | 0.53 | 4.95 | 1.67 | 1.24 | 0.11 | 2.91 | 5.34 | 121 | 37.18 | 46 | 28.30 |
| 93 | Qrg | 93-052 | 74.4 | 0.26 | 13.2 | 1.71 | | 0.04 | 0.33 | 1.27 | 3.63 | 4.22 | 0.09 | 0.25[7] | | | 99.40 | 75.17 | 0.26 | 13.34 | 1.55 | 0.04 | 0.33 | 1.28 | 3.67 | 4.26 | 0.09 | 7.93 | 4.66 | 121 | 32.30 | 46 | 29.22 |

*X-ray fluorescence analyses, except those otherwise noted, done in U.S. Geological Survey laboratory in Denver, Colo. (analysts, D.F. Siems and J.S. Mee)*

*FeO, $CO_2$, and water done in U.S. Geological Survey laboratories in Menlo Park, Calif. (analyst, N.H. Elsheimer) and Denver, Colo. (GR analyses: analysts, K.J. Curry and T.R. Peacock)*

*Analyses for field numbers prefixed by MK given in Korosec (1987) and done at Washington State University using XRF techniques; sample locations transferred from Korosec's field map may be slightly in error*

[1] *Analysis from Winters (1983) and done at Washington State University using XRF techniques; sample sites approximately located*

[2] *Analysis from Stine (1987) and done at Washington State University using XRF techniques; sample sites approximately located*

[3] *Located in Walupt Lake quadrangle just east of Hamilton Buttes quadrangle*

[4] *Located in Blue Lake quadrangle just west of Hamilton Buttes quadrangle*

[5] *Located in Green Mountain quadrangle a short distance south of Hamilton Buttes quadrangle*

[6] *Located in Packwood Lake quadrangle along Jordan Creek trail just north of Hamilton Buttes quadrangle*

[7] *LOI (Loss on ignition)*

[8] *No number 60*

*(Map unit in parentheses sampled in landslide)*

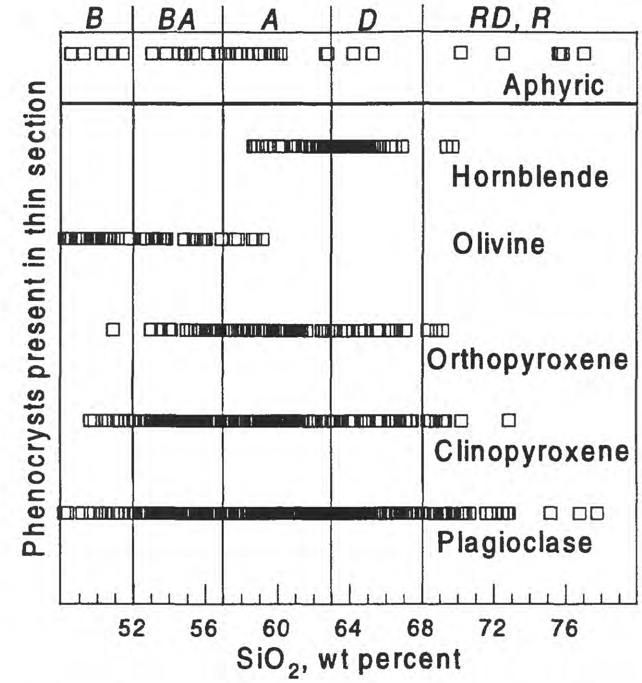


Figure 4. Plot of phenocryst assemblage vs. $SiO_2$ for 418 porphyritic and 39 non-porphyritic Tertiary rocks, chiefly in the seven mapped quadrangles but including a few in other quadrangles. □, phenocryst observed in thin section; Rock types along top edge from figure 3. Revised from less complete version in Swanson (1993). Modal amounts of phenocrysts range widely to a maximum of nearly 50 percent; typical values are 5–20 percent.

This index is notably less than the range of 61.8–63.1 for those in the previously mapped quadrangles. The Quaternary rocks, on the other hand, are clearly calcic, with a tightly defined alkali-lime index of 62.1 (fig. 7).

Most of the chemically analyzed Tertiary rocks, except those of the hornblende-bearing intrusive suite of Kidd Creek (H in figure 8) and a few others, are tholeiitic on a plot of FeO*/MgO vs. $SiO_2$, according to the classification of Miyashiro (1974). This pattern resembles that in the adjacent quadrangles. All of the Quaternary lava flows are calc-alkaline, except for the basalt of Walupt Lake volcano, which is slightly tholeiitic (fig 8). This continues the pattern for Quaternary rocks farther west, where only the least silicic basalt is tholeiitic and all other compositions are calc-alkaline.

All but one of the analyses are subalkaline on a plot of total alkalies vs. $SiO_2$ (fig. 9; Macdonald and Katsura, 1964; Irvine and Baragar, 1971). One of the Tertiary samples is mildly alkalic according to Macdonald and Katsura, but it is probably altered. The subalkaline character is stronger with increasing $SiO_2$ content, but even the least silicic Tetiary basalt is clearly subalkaline.

A plot of $K_2O$ vs. $SiO_2$ (fig. 10) shows that almost all samples with $SiO_2$ between 52 and 63 percent are medium-K mafic and silicic andesite according to Gill (1981; basaltic andesite and andesite, respectively, in the IUGS terminology used here). Silicic Quaternary rocks have high $K_2O$ contents, and Tertiary basalt is poor in $K_2O$, possibly owing to the accumulation of calcic plagioclase in these highly plagioclase-phyric rocks.

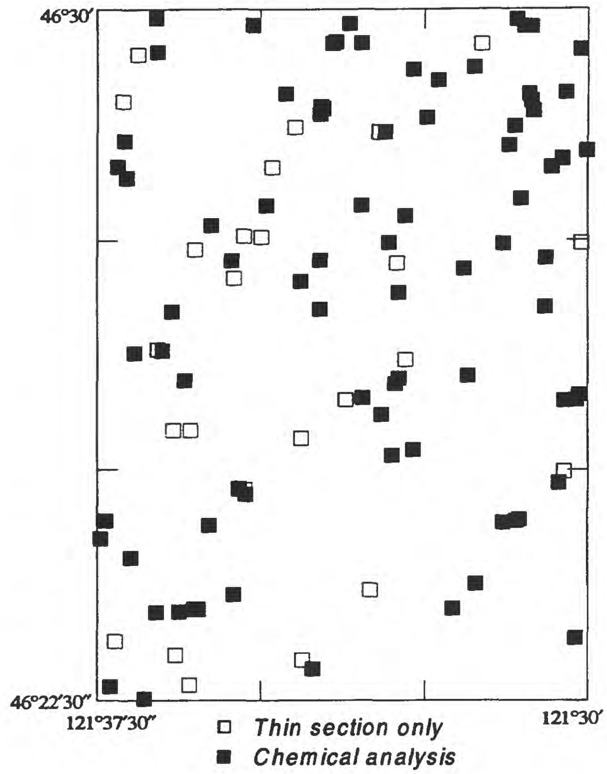


Figure 5. Map showing distribution of 116 sample localities in Hamilton Buttes quadrangle, including localities for analyzed samples collected by Korosec (1987), Winters (1983), and Stine (1987) and listed in table 1.

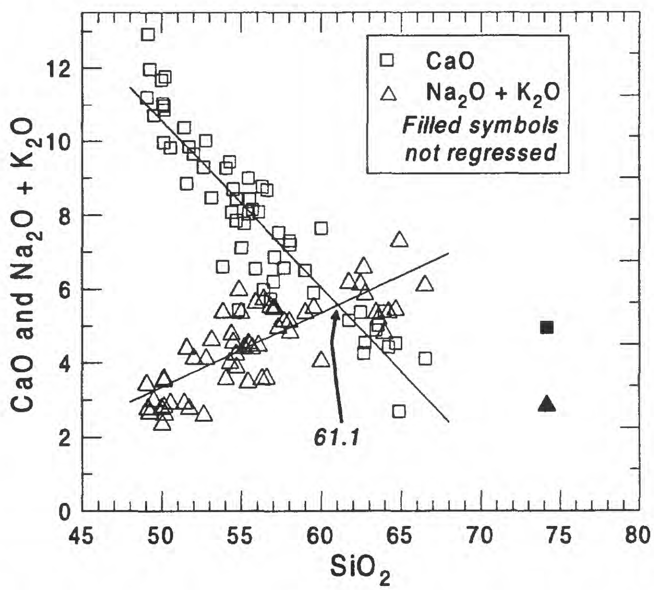


Figure 6. Plots of CaO and ($Na_2O + K_2O$) against $SiO_2$ for all analyzed Tertiary rocks in Hamilton Buttes quadrangle. Linear regressions of both plots cross at $SiO_2$ content of 61.1—slightly calcic in terminology of Peacock (1931). Filled symbols represent highly altered rock (table 1, no. 92) and are excluded from regressions.

## GEOLOGIC OVERVIEW OF QUADRANGLE

Bedded volcaniclastic rocks—principally volcanic sandstone but including mudstone, laharic deposits, and ash-flow tuff—of late Eocene and Oligocene age underlie most of the

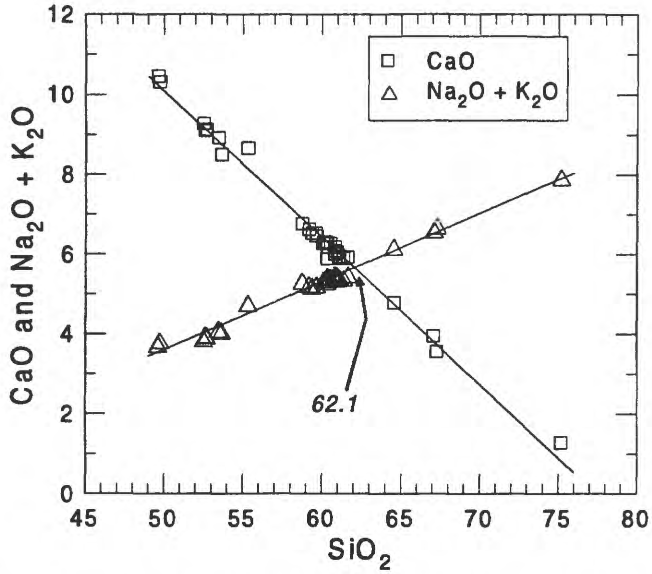


Figure 7. Plots of CaO and ($Na_2O + K_2O$) against $SiO_2$ for all analyzed Quaternary rocks in Hamilton Buttes quadrangle. Linear regressions of both plots cross at $SiO_2$ content of 62.1—calcic in terminology of Peacock (1931).

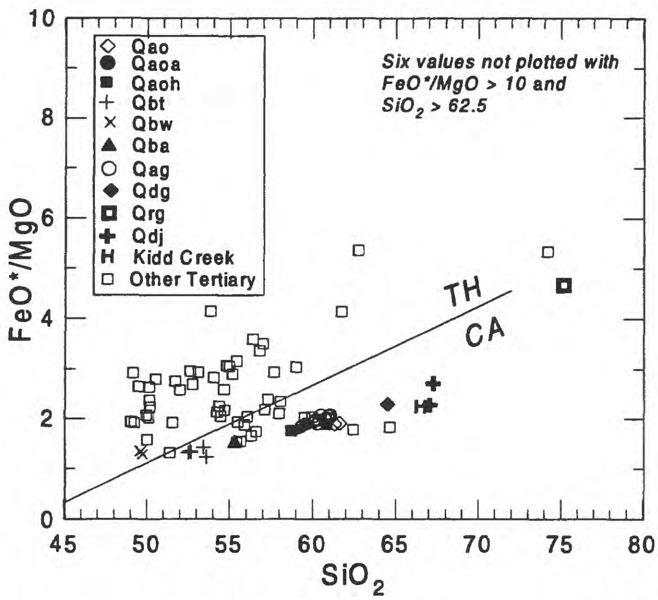


Figure 8. Plot of FeO*/MgO against $SiO_2$ for all chemically analyzed Tertiary and Quaternary rocks from Hamilton Buttes quadrangle. Subdivision into tholeiitic (TH) and calc-alkaline (CA) suites after Miyashiro (1974). Most Tertiary rocks are tholeiitic, but hornblende diorite of intrusive suite of Kidd Creek is clearly calc-alkaline, as are several older rocks. Quaternary lava flows are calc-alkaline, except for slightly tholeiitic basalt of Walupt Lake volcano. See caption of figure 3 for map-unit identifications of Quaternary rocks.

quadrangle. They overlie and are interbedded with a section of fluvial micaceous arkose 1–1.5 km thick that was derived from a moderate-grade metamorphic terrane in northeastern Washington.

Lava flows of andesite and basaltic andesite form a thick pile in the northeastern corner of the quadrangle but otherwise are uncommon. The flows may be part of a larger edifice centered a few kilometers farther north. Either a facies

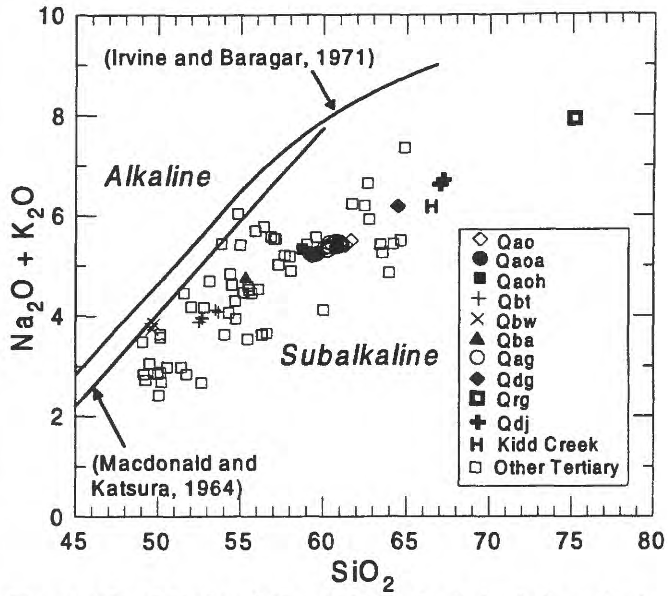


Figure 9. Plot of ($Na_2O + K_2O$) against $SiO_2$ for all chemically analyzed Tertiary and Quaternary rocks in Hamilton Buttes quadrangle. Boundaries shown between subalkaline and alkaline suites after Macdonald and Katsura (1964) and Irvine and Baragar (1971). Nearly all samples are decidedly subalkaline. Tertiary sample (table 1, no. 33) in alkaline field probably enriched in both $Na_2O$ and $K_2O$ during alteration. Analysis 92 not plotted. See caption of figure 3 for map-unit identifications of Quaternary rocks.

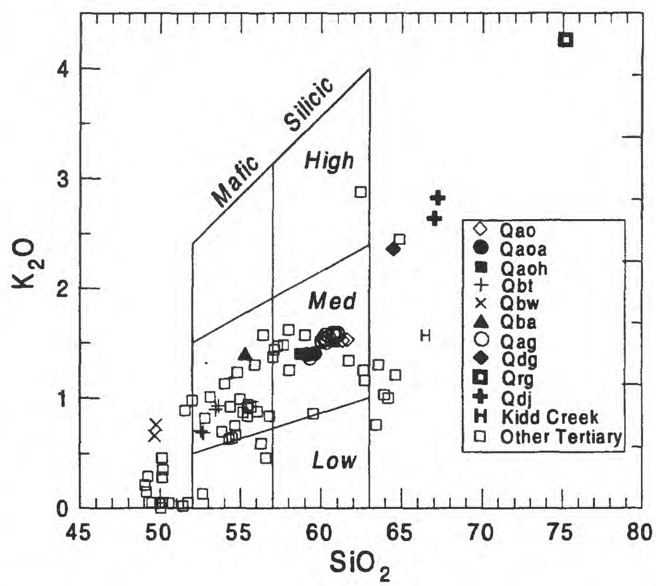


Figure 10. Plot of $K_2O$ against $SiO_2$ for all chemically analyzed Tertiary and Quaternary rocks from Hamilton Buttes quadrangle. Fields modified from Gill (1981), so that mafic andesite (basaltic andesite in IUGS terminology used in this paper) extends down to 52 percent. Note potassic nature of rhyolite of Goat Ridge (Qrg) and to lesser degree of dacites of Jordan Creek and Goat Ridge. Low-$K_2O$ nature of Tertiary basalt, mostly sills of Hugo Lake, also evident. Analysis 92 not plotted. See caption of figure 3 for map-unit identifications of Quaternary rocks.

change or an unrecognized fault separates the bulk of the section from the part dominated by lava flows.

The Tertiary section is intruded by numerous sills that range from basalt to mafic dacite but are mainly basalt and basaltic andesite. The sills can be subdivided into two map units on the basis of size and abundance of plagioclase phenocrysts. The sills are particularly numerous in the arkose but intrude higher parts of the section as well. A few dikes occur in each of two swarms, one trending northwest in the northwestern part of the quadrangle and the other trending east-northeast in the southwestern part.

After a period of folding and erosion, volcanism resumed in the late Pleistocene with the eruption of several different units of lava flows ranging in composition from silicic dacite to olivine basalt. All of the flows have normal magnetic polarity, and at least most are likely of Brunhes age. A center of andesitic volcanism lies on the west end of Goat Ridge in the northeastern part of the quadrangle. Flows from this center entered the drainages of Goat, Chambers, and Jordan Creeks. The youngest several eruptions of the Goat Rocks volcanic center, a Pliocene–Pleistocene center a few kilometers northeast of the quadrangle, produced andesite flows that advanced down Goat Creek and the Cispus River into the quadrangle. These flows are likely about 0.14–0.02 Ma, as is most of the basalt erupted in the southeastern part of the quadrangle and farther east.

The area was extensively glaciated during the late Pleistocene. Till of Evans Creek Drift covers much of the eastern third of the quadrangle. Several extensive landslides postdate the glaciation. Lakes resulting from glaciation and landsliding are common.

## TERTIARY ROCKS OLDER THAN INTRUSIVE SUITE OF KIDD CREEK

**Arkose of Chambers Creek (map unit Tsc)**—Well-bedded, generally micaceous arkose and lesser pebble conglomerate, siltstone, and mudstone are the oldest rocks in the quadrangle. They crop out primarily on the west flank of the Johnson Creek anticline, from the northern edge of quadrangle to east of the mouth of Chambers Creek. The arkosic rocks occur less extensively on the east limb of the anticline, where they are poorly exposed owing to a cover of Quaternary lava flows and till. (For discussion of this puzzling area, see the section on folds in this paper.) Unpublished mapping shows that the unit extends only slightly north of the quadrangle but at least 1.5 km south, where it crops out along Wesley Creek and in cuts along an abandoned road 1 km north-northwest of Midway Meadows. Some of the best and most accessible exposures are along Forest Service (FS) road 22 that climbs the west side of Chambers Creek valley. Other especially good exposures are in the upper reaches of the North Fork Cispus River and in scattered road cuts along FS 21 north and south of Hugo Lake.

Winters (1984) was the first to make a detailed study of these rocks, which he termed the *Chambers Creek beds*. He mapped much of their distribution and conducted an excellent petrographic and sedimentologic analysis of them. He found (p. 1–2) that the

> ...Chambers Creek beds are dominated by fine-grained strata. Mudstone, siltstone, and very fine-grained arkosic sandstone form 10 to 19 meter thick coarsening-upward intervals interpreted as nonmarine regressive sequences.
>
> Lateral to, and intercalated with these fine-grained intervals are thick, relatively coarse-grained sand bodies, characterized by half meter- to meter-scale planar and trough cross bedding. Paleocurrent patterns, sand body geometry, and fining-upward intervals indicate these originated in a nonmarine channel environment.
>
> The intercalation of regressive and channel sequences implies a common depositional setting. The former probably originated by infilling of lakes or lagoons adjacent to major distributaries. The latter represent deposition in and adjacent to these paleochannels. The thickness of the regressive cycles, their rarity of emergence, and the low width-depth ratio of the channels suggest rapid basin subsidence.

Much of the micaceous sandstone is cross bedded, typically on a fine scale in beds no more than several tens of centimeters thick. Channels are numerous but shallow. Ripple-marked bedding planes are common in fine-grained sandstone and siltstone, probably overbank and bar deposits. A photogenic example of a ripple-marked sandstone is in a cut along the North Fork Cispus road (FS 22) (lat 46°27.37′, long 121°34.56′).

Pebble conglomerate occurs in some of the channels. It typically contains moderately well-rounded to well-rounded clasts of volcanic rocks that resemble those in overlying and interbedded (see below) volcaniclastic rocks. Thin sections show that the pebbles are typically dacite or rhyolite low in the section but predominantly andesite and even basalt high in the section. A good place to see the silicic pebble conglomerate is in cuts along a logging road at an elevation of 4310 ft on the west side of upper Johnson Creek (lat 46°28.72′, long 121°34.45′). Andesitic pebble conglomerate is well exposed in cuts along FS 22 (lat 46° 27.54′, long 121°35.00′), near the top of the arkosic section.

The pebble conglomerate, though not voluminous, is important, for it shows that the volcanic arc was probably active during deposition of the arkose. Most of the clasts are fresher than the pre-arc volcanic rocks in central Washington, another potential source of the clasts. Rhyolite similar to that in the silicic pebble conglomerate occurs near the base of the arc section (Ohanapecosh Formation) along Summit Creek, 12 km northwest of White Pass (Vance and others, 1987); it could be the parent for some of the silicic clasts.

More convincing evidence of contemporaneous deposition of arkose and volcaniclastic arc detritus is the presence of volcanic sandstone, tuff, and mixtures of arkosic and volcaniclastic detritus throughout the arkosic section. In some beds, the detritus is mixed on the scale of a thin section; in others, the detritus may lack volcanic influence or have a wholly volcanic source. Winters (1984) interpreted the interbedding and mixing to be confined to the upper 600 m of section, below which is at least 600 m of pure arkose. I agree that the lower half of the section consists mainly of arkose but found many beds composed of a mixture of arkosic and volcaniclastic debris, including fragile pumice clasts, and a few that consist almost entirely of arc detritus. The geologic map shows where these beds were identified in the field; some field observations were confirmed by thin-section inspection. Beds of pure or nearly pure micaceous arkose are common throughout the section, in places even interbedded with volcanic sandstone. Cuts along the North Fork Cispus road (FS 22) show an eye-catching example of white, nearly pure arkose at the top of the section (lat 46°27.54′ long 121°35.00′).

Winters (1984) showed that cross bedding and current ripples "indicate generally westward to southwestward paleoflow" (p. 85). He found similar current directions in the interbedded volcanic sandstone high in the section, as did Stine (1987) for fluvial volcaniclastic rocks just upsection from those studied by Winters. My general observations agree with the measurements by Winters and Stine.

Joe O'Connor (U.S. Geological Survey) studied the heavy mineral suite in two samples of arkose from high in the section in the North Fork Cispus drainage (table 2), using techniques described in Johnson and O'Connor (1994; see also O'Connor, 1992). He interprets the suite to indicate a provenance in moderate-grade metamorphic rocks such as those east of the Straight Creek fault in northern and northeastern Washington and northern Idaho. Kyanite was looked for but not found; its presence in roughly coeval arkose farther north and west defines a river system flowing southwestward from a source region clearly not tapped by the arkose of Chambers Creek (Vance, 1989; J.A. Vance, oral commun., 1995).

The current directions and interpreted source region are consistent with one another. They clearly indicate a source beyond the eastern limit of the Cascade Arc, perhaps in the area suggested by O'Connor or in equivalent rock types now buried by the Columbia River Basalt Group on the Columbia Plateau. The dominant mineralogy of the arkose—quartz, chert, alkali feldspar, and muscovite (Winters, 1984)—likewise suggests derivation outside the arc. The current directions also indicate a general westward river flow in the interbedded and overlying volcanic sandstone, even after the supply of arkosic debris was cut off.

Table 2. Heavy mineral content (by volume) of two samples of arkose of Chambers Creek. Courtesy J.T. O'Connor (oral commun., October 1994).

| Mineral | Percent heavies | |
|---|---|---|
| | *Sample 46S* | *Sample GP8* |
| Zircon | 3.3 | 2.3 |
| Epidote | 33.2 | —— |
| Zoisite | 1.2 | —— |
| Sphene | 46.1 | 81.3 |
| Allanite | 4.2 | 0.5 |
| Garnet | 6.2 | 6.1 |
| Apatite | 4.2 | 5.6 |
| Rutile | 0.4 | 1.9 |
| Staurolite | 0.4 | —— |
| Kyanite | 0 | 0 |
| Tourmaline | 0.8 | 0.9 |
| Monazite | —— | 1.4 |
| Total | 100.0 | 100.0 |

***Significance of interbedded arkose and volcanic sandstone***—The section of arkose and interbedded volcanic sandstone is about 1.5 km thick, a slight upward revision of the figure in Swanson (1994b). This figure was calculated from an outcrop width of about 3 km and an average dip of 40°, subtracting 300–400 m for younger sills (see section on intrusions). The thickness of the sills might be overestimated by 25–50 percent. To explain the straight west side of Chambers Creek and upper coarse of Johnson Creek, an unrecognized fault (Winters' [1984] *Hugo Lake lineation*) could lie at the base of the ridge, though my preferred interpretation is that this is simply a strike ridge. The section west of the putative fault is about 1 km thick (outcrop width about 2 km) after sills are subtracted. Thus the true thickness of the Chambers Creek and interbedded volcanic sandstone and siltstone is 1–1.5 km, most likely about 1.5 km.

The interbedded relations almost demand coeval volcanism and arkosic sedimentation. The volcaniclastic detritus is fresh—not reworked from older, pre-arc rocks. This is indicated by the presence of fragile pumice and airfall ash scattered throughout the section. Moreover, most of the volcanic debris is andesite and dacite similar to that in the overlying volcanic sandstone, not altered basalt such as that which dominates older Eocene units farther north.

Subsidence at a rate subequal to that of sedimentation is the best way to account for the 1–1.5–km–thick section of fluvial, mostly low-energy deposits. The arkosic detritus was carried by one or more rivers from the craton to the site of deposition, which was therefore not an isolated basin entirely within the arc. Such drainage continued into and across the depositional basin as the thick section developed. This could reflect ongoing uplift of the cratonic source. More likely, however, the interbedded section records subsidence along the nascent arc, trapping and mixing far-traveled cratonic debris with volcaniclastic detritus (and minor airfall ash) shed from neighboring active volcanoes.

Probably the river system made its way across the subsiding axis of the young arc and supplied some of the sediment now forming the marine sandstone of the Cowlitz Formation of southwestern Washington and northwestern Oregon (Henriksen, 1956; Roberts, 1958; Armentrout and Suek, 1985; Evarts and Swanson, 1994, p. 2H-12). The Cowlitz Formation contains kyanite (Vance, 1989), however, and so was also supplied by a more northerly river system than that which deposited the kyanite-free arkose of Chambers Creek. As is the Chambers Creek, the Cowlitz is dominantly arkosic sandstone and siltstone but contains increasingly abundant arc detritus near the top of the section and eastward toward the arc (Evarts and Swanson, 1994, p. 2H-12–2H-13).

Is this an isolated instance of early arc subsidence in the southern Washington Cascades? It is certainly the most convincing, but two other sections of Eocene arkose contain interbeds of volcanic sandstone.

Evarts and others (1983b) described interbeds of the early-arc, volcaniclastic Ohanapecosh Formation in micaceous arkose of the Spiketon Formation in a section 120 m thick just west of Mount Rainier National Park, 30 km north of Randle (fig. 1).

Clayton (1983) and Vance and others (1987) reported about 850 m of late Eocene micaceous arkose along Summit Creek, 12 km northwest of White Pass (fig. 1). They found that the upper 100 m of the Summit Creek section contains interbeds of, and is mixed with, the Ohanapecosh, though the lower 750 m is free of arc debris.

Near Morton, Johnson and Stanley (1995) described the 42–Ma Northcraft Formation, probably an early Cascade arc unit, as interbedded in a 400–m–thick section with arkosic deltaic deposits. This relation is similar to that at the other localities of interbedding, although the volcaniclastic rocks are somewhat older.

In and southeast of Mount Rainier National Park, Fiske (1963) interpreted the Ohanapecosh Formation to have been deposited subaqueously, primarily by pyroclastic flows possibly erupted under water. Vance and others (1987, p. 278) questioned this interpretation and believe much of the formation comprises subaerial "airfall debris and mud flows". No matter which depositional environment is correct, the thickness of the mostly volcaniclastic section, about 3 km, would imply ongoing subsidence during deposition of much of the Ohanapecosh. Regional reconnaissance work (Hammond, 1980; Swanson and Clayton, 1983) suggests that the Ohanapecosh Formation in the southeastern part of Mount Rainier National Park and along the White Pass highway (the section studied by Fiske [1963; Fiske and others, 1963] and Vance and others [1987]) is about the same age as the upper part of the Chambers Creek and overlying volcaniclastic rocks in the Hamilton Buttes quadrangle.

Thus there are tantalizing suggestions that early arc volcanism in southern Washington was accompanied by subsidence, which for some time allowed rivers to just keep pace with the growing thickness of the arc.

What is the age of this subsidence? Winters (1984) reported a zircon fission-track age of 35.9 ± 0.7 Ma for an airfall tuff near the middle of the section (plate 1); this is the only numerical age for the Chambers Creek. Winters thought the age is too young on the basis of regional considerations of the age of other arkose in central Washington, and so he ascribed it to thermal resetting. Joe Vance, who supervised the counting of Winters' sample, found no evidence in the zircon crystals for reheating (J.A. Vance, oral commun., 1994). Consequently I think it most likely that the age is reasonable and simply dates a somewhat younger period of arkosic deposition than has heretofore been recognized.

Vance and others (1987) obtained three zircon fission-track ages of about 36 Ma from rhyolite in the lower part of the Ohanapecosh Formation, just above the 100–m–thick section of interbedded volcanic sandstone and arkose along Summit Creek. These ages agree with that from the Chambers Creek section. However, arkosic sedimentation continued for a longer time in the Chambers Creek area, where at least 500 m of section occurs above the dated tuff.

If these ages and attendant reasoning are correct, subsidence and volcanic activity in the arc began somewhat before 36 Ma, perhaps 38 Ma or so, in both the Chambers Creek and Summit Creek areas. By about 36 Ma, rivers carrying arkosic sediment were excluded from the Summit Creek section by developing topography but continued flowing through the Chambers Creek area. Not until perhaps 35–34 Ma or even later did volcaniclastic deposition outpace subsidence in the Chambers Creek area, as the arc became a positive landform. Subsidence must have continued, however, to accomodate 4–5 km or more of volcaniclastic rocks that eventually accumulated in the section (Swanson, 1993; Evarts and Swanson, 1994).

***Relation to SWCC***—Stanley and others (1987) suggested that the conductivity anomaly beneath the southern Washington Cascades represents a buried early Tertiary accretionary wedge. Later, Stanley and others (1992) proposed that the SWCC comprises Eocene marine mudstone above a Late Cretaceous to Paleocene accretionary wedge.

Another possibility is that the conductivity anomaly reflects water-rich sedimentary rocks that are marine equivalents of the fluvial arkose of Chambers Creek. This alternative has the attraction of not needing an accretionary wedge, which is not exposed or strongly suggested by surface geology or other subsurface geophysics. What is the evidence for such an interpretation?

Independent of this study, Johnson and Stanley (1995) described nonmarine and interbedded marine arkose and mudstone in the Morton anticline—a faulted uplift near Morton (fig. 1). They correlated this section with the Carbonado Formation and suggested that the marine facies of the section may form part or all of the SWCC. Johnson and Stanley (1995, p. 291) interpret the Carbonado near Morton as having "accumulated within a river- and tide-influenced delta." Perhaps the Chambers Creek is the upstream facies of the river system that supplied sediment to the delta and over time prograded westward across a marine basin. Sediments depositing in this basin may define part of the SWCC. The SWCC is more than 8 km thick. If composed entirely of marine sedimentary rocks, it would record major syndepositional subsidence in one or more basions, perhaps in a transtensional setting as Johnson and Stanley envision. However, detailed seismic refraction studies suggest that the seismic velocity of the lower part of the SWCC near Morton is too high to be caused by most sedimentary rocks (Kate Miller, oral commun., 1995). Hence the SWCC may be a composite, much as Stanley and others (1992) suggested, with the marine mudstone being a thick, fine-grained facies of the Chambers Creek and Carbonado units and the underlying high-velocity rocks an accretionary wedge.

**Volcaniclastic rocks (map unit Ttv)**—Bedded volcaniclastic rocks of various origins underlie most of the quadrangle. They are particularly well exposed in the Hamilton Buttes-Elk Ridge area, where they form prominent ledges traceable for hundreds of meters through early 20th–century burns that have not yet grown back. The outstanding exposures in the Hamilton Buttes area prompted Stine (1987) to undertake a sedimentologic study of the bedded volcaniclastic rocks. Elsewhere, nearly inaccessible cliffs along Stonewall Ridge are carved into the unit. Cuts along the North Fork Cispus road (FS 22) show a variety of rock types and illustrate the interbedded nature of the volcaniclastic rocks with the arkose of Chambers Creek.

Included in the unit are: 1) epiclastic rocks, such as volcanic sandstone, siltstone, and conglomerate, eroded from penecontemporaneous volcanic rocks or unconsolidated deposits and transported by streams; 2) pyroclastic rocks, such as bedded airfall tuff and lithic-lapilli tuff of ash-flow origin, deposited directly by eruption-related processes, and 3) lithic and (or) pumiceous diamictite whose origins are uncertain but most likely result from debris flows (lahars) fed either directly by eruptions or by somewhat later, but fundamentally volcano-related, erosional processes. These rock types dominate the section.

The epiclastic suite consists entirely of clasts either eroded from slightly older Cascade volcanic rocks or reworked from deposits of contemporary eruptions. Clasts range in grain size from silt to gravel but are predominantly medium to coarse sand. Pebble and cobble conglomerate comprised entirely of volcanic clasts is locally prominent, as in places on the west flank of Elk Ridge and near the top of the ridge just north of St. John Lake. Wide ranges in degree of sorting and rounding characterize the deposits; in many places, well-sorted volcanic sandstone is interbedded with poorly sorted rocks including even diamictite with a matrix-supported framework. Beds range in thickness from less than 1 cm to more than 50 cm, averaging a few centimeters. Channels and lensoid beds are especially common. Cross bedding is locally apparent and typically indicates a general east to west transport direction, as documented by Stine (1987) and Winters (1984). Poorly preserved plant remains occur in many beds and along bedding planes.

The pyroclastic suite is dominated by lithic-lapilli tuff and lithic-pumice lapilli tuff, most of which is probably of ash-flow origin. A dirty white welded tuff with a formerly vitrophyric base crops out at 5500 ft elevation just north of St. John Lake (table 1, no. 91); this welded tuff might correlate with a similar tuff along strike near the top of Cold Springs Butte, 1.3 km west of St. John Lake in the Blue Lake quadrangle (Swanson, 1993, table 1. no. 81). Overall, however, welding is uncommon, and distinguishing a nonwelded primary pyroclastic flow from a pumiceous or even lithic lahar is difficult. Lithic-lapilli tuff and pumice-lapilli tuff commonly intertongue with other volcaniclastic deposits but are not nearly as abundant as the epiclastic and laharic deposits. They are most common along the western edge of the quadrangle and overall are more abundant than epiclastic and laharic deposits in much of the area farther west that I have previously mapped. Air-fall tuff is easily misidentified as epiclastic mudstone, and in fact much of the mudstone could be reworked or even *in situ* tuff.

Lithic diamictite is an important rock type in the upper half of the section. It occurs in beds from a few centimeters to a few meters thick and is typically supported by matrix but locally by clasts. Subrounded boulders tens of centimeters in diameter are fairly common, though the dominant size is in the pebble or cobble range. Many beds contain fragments of wood, including limbs or trunks a few centimeters or more in diameter. Some beds of diamictite contain much pumice, though most are almost entirely lithic. Generally the upper and lower surfaces of a bed are almost planar, but in places one or both may be irregular, probably because of erosion. Most of the diamictite doubtless formed from volcanic debris flows (lahars), but locally some could be colluvial or landslide deposits.

All of the bedded rocks in the quadrangle were apparently deposited in lowlands rather than on the flanks of cones. This conclusion, also reached by Stine (1987) and by me (Swanson, 1993) for the bedded rocks in the adjacent Blue Lake quadrangle, is supported by the observation that bedding attitudes are nearly everywhere consistent with local structure and hence were probably subhorizontal when deposited. Many of the deposits, such as sandstone and conglomerate, were clearly deposited by streams, just as expected in the "alluvial apron" setting envisioned by Stine (1987) or the intermediate to distal fluvial facies described by Smedes and Prostka (1972), Kuenzi and others, (1979), Vessell and Davies (1981), and Smith (1987). The thick accumulation, perhaps 4.5–5 km, of alluvial-apron volcaniclastic rocks in this and the mapped quadrangles farther west is consistent with the concept of syndepositional subsidence as the volcanic pile accumulated (Swanson, 1993; Evarts and Swanson, 1994).

**Lava flows (map unit Ta)**—Few lava flows crop out in the quadrangle, in contrast to their relative abundance in the previously mapped quadrangles farther west. Two thin, nearly aphyric andesite flows occur near St. Michael Lake; the northern of the two is rubbly in places and ends just inside the Blue Lake quadrangle, where I overlooked it when preparing the geologic map (Swanson, 1993). A thin, platy andesite flow, slightly and finely plagioclase phyric, is poorly exposed just north of Timonium Creek. These bodies have vesicular (now mostly amygdaloidal) flow tops, so they are not sills; otherwise they closely resemble some of the numerous sills in the area.

Aphyric to moderately pyroxene-plagioclase-phyric andesite and basaltic andesite lava flows unconformably underlie Quaternary andesite on Goat Ridge east of the crest of the Johnson Creek anticline. The flows, in which veins of quartz and calcite are common, overlie volcanic sandstone and interbedded minor arkose 1 km northeast of Chambers Lake. Farther northeast, the flows are interbedded with tuffaceous volcanic sandstone and lithic-lapilli tuff or laharic diamictite in a belt crossing Goat Ridge. Sills intrude the flows and volcaniclastic rocks; in places determining whether a particular outcrop is in a flow or sill is largely guesswork.

This section of lava flows, at least 1 km thick on Goat Ridge, extends northwest along strike into the Packwood Lake quadrangle, where it may merge into an eruptive center on and north of Angry Mountain (Swanson and Clayton, 1983; my currently unpublished detailed mapping). The section of lava flows on Goat Ridge may underlie the distal flank of a large volcano or a lowland near the volcano.

In earlier reconnaissance, I mapped the extreme northeastern part of the thick flow section (northeast of the sills) as part of an intrusion (Swanson and Clayton, 1983; Church and others, 1983). This interpretation was based on lack of observed vesicular zones, relatively coarse grain size of some of units, and lack of obvious contacts. This area remains confusing, but in more detailed work I have found probable amygdules of epidote and chlorite. The problematic rock has been thermally metamorphosed, with epidote abundant in plagioclase phenocrysts, and this obscures details of contacts. Nonetheless, abrupt changes in grain size occur that I now interpret as flow contacts. Moreover, platy jointing at several places east of the Goat Ridge trail closely resembles ramp structures and other platy features of andesite lava flows. Consequently I now interpret these rocks as lava flows. Certainly more work in this and adjacent areas is needed to resolve the origin of the andesite.

**Intrusions**—Intrusions are common in the quadrangle, particularly sills. They are probably older than the intrusive suite of Kidd Creek, as judged from evidence found in the other mapped quadrangles. However, in general only their ages relative to their host rocks are known, and age relations among the different intrusions in the quadrangle are completely unknown.

***Dikes***—The 33 mapped dikes of andesite and basaltic andesite are concentrated in two sets, each with a distinctive trend and map location (figs. 11 and 12*B*). The dominant set (21 dikes) occurs between Wobbly Lake and the northwest corner of the quadrangle. Most dikes in this set strike about 320° but range from 290° to 340°. These dikes form part of a set that is well developed in the northeastern quarter of the Blue Lake quadrangle (fig. 11; Swanson, 1993). The dikes contain sparse to moderate amounts of plagioclase phenocrysts. Dikes on the east side of Stonewall Ridge dip steeply, typically about 75–80° northeast. Rotation of bedding back to horizontal restores a nearly vertical dip to the dikes, which therefore probably predate folding.

Three dike segments along the top of Stonewall Ridge (possibly erosional remnants of only one dike) have an unusual 30° strike and dip only 65° east. Rotation of bedding back to horizontal makes the dikes subvertical. Owing to their relatively shallow dip, the dike segments locally define closed map patterns like necklaces around high points along the ridge crest. The andesite in the dikes contains abundant large plagioclase phenocrysts and is replete with zeolite and calcite veins and amygdules. A chemical analysis of one of the dike segments (table 1, no. 2) has very high $Al_2O_3$ and CaO reflecting the abundant large plagioclase phenocrysts; in this regard the dike is chemically similar to, and possibly correlative with, the most mafic of the sills of Hugo Lake (map unit Taih). Steeply plunging slickensides score the contacts of the dikes with the host rock in many places. These features physically distinguish the northeast-striking dikes from the northwest-striking dikes in this part of the quadrangle.

The second set of 12 dikes or dike remnants occurs only near Hamilton Buttes, except for two thick dikes along the western edge of the quadrangle west and southwest of Wobbly Lake. Most dikes in this set strike about 60° and contain a few percent of plagioclase phenocrysts. The dikes are typically only 1–3 m wide, although the two that extend into the Blue Lake quadrangle are as wide as 60 m in places (Swanson, 1993).

The intrusion on Hamilton Buttes itself is a multiple dike, with several narrow, discontinuous screens of fine-grained diamictite separating different dikes. Excellent exposures show that the east end of the body clearly crosscuts bedding. The multiple dike reaches a maximum width of 200 m and is relatively coarse grained, even microdioritic. Such grain size suggests that the different segments intruded and cooled as essentially one body; otherwise, individual dikes would be fine-grained despite the overall width of the body. The uniformity of composition likewise suggests that the individual dikes were emplaced from one magma body (table 1, nos. 38, 40, 43, and 45).

The thick dike 1.5 km north-northwest of Mud Lake bends southward just inside the Blue Lake quadrangle and re-enters the Hamilton Buttes quadrangle to form the gently dipping, cross-cutting but almost sill-like, dike 700 m north of Mud Lake (Swanson, 1993). The bend and both limbs of the dike are well exposed in the Blue Lake quadrangle, so there is little doubt of the complex form of the intrusion. The consistency of chemical composition (table 1, nos. 28–30) further supports the presence of only one geometrically complex body.

One andesite dike is far removed from either of the two sets. It cuts fine-grained volcanic sandstone along Jordan Creek near the north edge of the mapped area. The dike is 2 m wide and contains numerous plagioclase phenocrysts. It strikes 340° and dips only 70° west. Rotation of the host sandstone, which dips 25° east and strikes 340°, back to horizontal makes the dike subvertical; hence the dike probably predates folding. The dike could be an offshoot of one of the numerous sills in this area, although most of them contain only a few plagioclase phenocrysts.

***Sills (map units Taih and Tai)***—Sills of andesite, basalt, and less common diabase and microdiorite riddle the bedded rocks in the quadrangle. They are especially abundant low in the section, chiefly in the arkose of Chambers Creek, but occur higher in the section as well. The sills can be subdivided into two sets on the basis of rock type as observed in the field.

*SILLS OF HUGO LAKE.* Highly and commonly coarsely plagioclase-phyric basalt, basaltic andesite, and lesser diabase and microdiorite form numerous sills (map unit Taih; table 1, nos. 1, 4, 7, 9–11, 15, 17, 22–23, 34–35, and 48) cutting the arkose of Chambers Creek and the stratigraphically higher volcaniclastic rocks. The sills are most abundant in the Chambers Creek section. There they form linear strike ridges, many of which are obvious on the 40–foot contour map, that stand above the sedimentary rocks owing to glacial erosion. Some sills can be easily traced along strike ridges

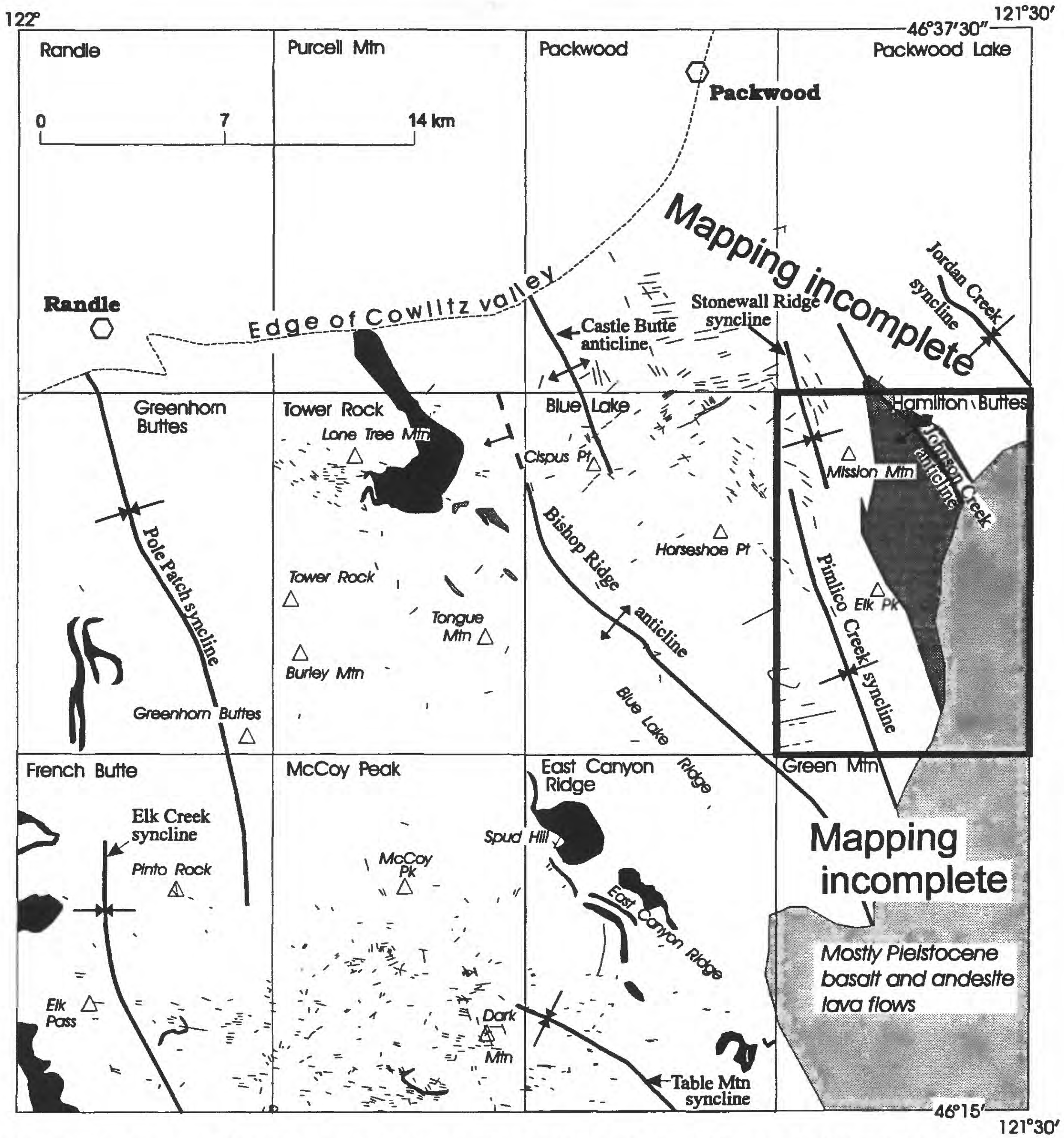


Figure 11. Generalized distribution of pyroxene andesite and basaltic andesite dikes (short lines), arkose of Chambers Creek (dark shade), and dacite and rhyolite extrusions and intrusions (black) in mapped quadrangles south of Cowlitz River. Hamilton Buttes quadrangle heavily outlined. Dikes in Packwood and Packwood Lake quadrangles shown schematically and incompletely. Axial traces of major folds also shown. Note right-stepping pattern of three major fold pairs: Pole Patch-Elk Creek syncline, Bishop Ridge-Castle Butte anticline, and Pimlico Creek-Stonewall Ridge syncline.

for 2 km or more. The sills range in thickness from a few centimeters to ten or more meters, generally 4–7 m. A typical sill is columnar jointed. The columns are perpendicular to the top and bottom of the sill; the orientation (azimuth and plunge) of the columns forms a reliable proxy for the complement of the dip. Many of the columns are cut by cross joints that approximate the attitude of bedding. Phenocrysts of plagioclase 3–6 mm long, and a few glomerocrysts as much as 10 mm or more across, typically form 10–30 volume per cent of the rock. Phenocrysts of two pyroxenes (both augite and hypersthene) generally make up a few per cent of each sample. From glassy (now devitrified) or very fine-grained margins, the grain size increases toward the interior of each sill, commonly reaching 1–2 mm in the coarsest microdiorite.

The wide range in compositions (49–57 percent $SiO_2$) suggests a complex petrologic assemblage included within the map unit. Some rocks rich in both $Al_2O_3$ and CaO are probably plagioclase cumulates, whereas others less rich in those components may record little differential movement of crystals and melt. The basaltic compositions are characterized by low amounts of $K_2O$ (fig. 10), perhaps reflecting accumulation of calcic plagioclase.

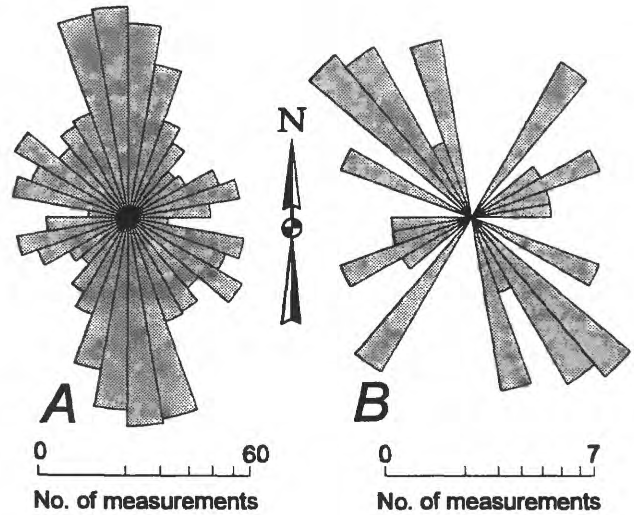


Figure 12. Equiarea rose diagrams in 10° increments showing strikes of bedded rocks and pyroxene andesite dikes in Hamilton Buttes quadrangle. *A*, 366 strikes of bedding (mean direction, 348°; s.d., 64.7°); *B*, 33 pyroxene andesite dikes; mean direction of 320.4° (s.d., 46.3°). Bar indicates number of measurements and is not linear because of *equiarea* style of plot.

Good examples of the sills of Hugo Lake are exposed in a large quarry on the east shore of the lake (table 1, nos. 34 and 35), in several cuts along the road (FS 22) that climbs west out of Chambers Creek valley (table 1, nos. 15 and 22–23), and along that same road in the North Fork Cispus drainage (especially in the cut at lat 46°27.46′, long 121°34.73′). The sill underlying Point 5975 in the northeast corner of the quadrangle (table 1, no. 17) is another good example, although quite isolated from other similar sills.

At least three coarse-grained sills of basaltic composition crop out in the North Fork Cispus valley, west of Wobbly Creek and east of the mouth of St. Michael Creek (table 1, nos. 3, 8, 12, and 42). These gabbro bodies (map unit Tg) chemically resemble the more mafic sills of Hugo Lake type and may simply be coarser varieties. The intrusion east of the mouth of St. Michael Creek has a wide range in composition, judging from the two analyses done in the same laboratory.

*SPARSELY TO MODERATELY PLAGIOCLASE-PHYRIC SILLS.* These sills (map unit Tai) of basaltic andesite and andesite, with lesser basalt and mafic dacite (table 1, numerous analyses) are less common than the sills of Hugo Lake but probably constitute more volume, because they form thicker bodies. This unit, found throughout the Tertiary section, includes most of the large sill complex of silicic andesite and mafic dacite east of Johnson Creek (best seen in a quarry 1.5 km south of the mouth of Jordan Creek) (table 1, nos. 80, 82–85), two extensive dip-slope exposures southwest (table 1, no. 26) and northwest (table 1, no. 16) of Chambers Lake, the two lower sills in the rugged northeast corner of the quadrangle (table 1, nos. 49 and 51), and the sill forming the lip of the cirque at St. John Lake at the south end of Stonewall Ridge (table 1, no. 52). In addition, smaller bodies are distributed throughout the quadrangle, most notably in the Wobbly Creek, North Fork Cispus, and St. John Creek drainages. Several sills are poorly exposed and could be dikes; two examples are the bodies east of Wobbly Creek from which analyses 27 and 31 (table 1) were obtained.

Sills of the unit are typically several meters to 50 m thick and columnar. Some are coarse enough to have a granular texture and could be called microdiorite, but the thinner bodies are fine-grained andesite and basaltic andesite. Some sills near one another may be members of a single body. For example, the similar compositions (table 1, nos. 49 and 51) and petrography of the two lower sills in the northeast corner of the quadrangle suggest fundamentally one unit despite the substantial thickness of volcaniclastic rocks between.

The unit is distinguished from the sills of Hugo Lake by its lower content of plagioclase phenocrysts (typically only a few percent, and in places almost nonporphyritic). Some sills have intermediate phenocryst contents that make their unit assignments arbitrary, but most fall neatly into one of the units.

The distinction on the basis of phenocryst abundance is clearer in the Hamilton Buttes quadrangle than in the other mapped quadrangles. In general, most of unit Tai in the other quadrangles would correspond to the unit in the Hamilton Buttes quadrangle, but some would be sufficiently porphyritic to resemble the sills of Hugo Lake.

Most sills of unit Tai are more silicic than most sills of Hugo Lake (fig. 13), and at least one thick and voluminous sill of unit Tai, best exposed in the quarry south of Jordan Creek (table 1, nos. 80, 82–83, and 85), is mafic dacite. One highly plagioclase-phyric dike on Stonewall Ridge (table 1, no. 2) is chemically like the most mafic sill of Hugo Lake and is likely an offshoot of one of those sills; it is shown as a dike of unit Tai on the geologic map.

The age relations between the two units of sills are unclear. Only in one place—on the crest of the ridge 400 m southwest of Chambers Lake—was the contact between the two units almost exposed (to within a few centimeters). Here, the sill of unit Tai is fine-grained against the sill of Hugo Lake and coarsens away from the contact; the Hugo Lake shows no textural change next to the contact. At this locality the less porphyritic sill is clearly younger. Generalizing this observation to all of the sills is risky, but it makes some sense that the Hugo Lake unit is mostly or entirely older. Hugo Lake sills might have physically and thermally "toughened" the arkosic section, making it less susceptible to later intrusion. Perhaps this is why the Hugo Lake unit is far more abundant than unit Tai in the Chambers Creek section.

***Other intrusions***—Two wide intrusions cut their host rock steeply but are not dikes in the usual sense of the term. The basaltic andesite intrusion south of St. Michael Lake (map unit Taim) is less well exposed than its continuation in the Blue Lake quadrangle but covers a slightly greater area (Swanson, 1993). The intrusion has steep contacts with, and locally deformed, the host volcaniclastic rocks. The basaltic andesite is highly jointed, fine to medium grained, and generally has a finely seriate texture. Chemical analyses are given in Swanson (1993, table 1, nos. 24 and 25).

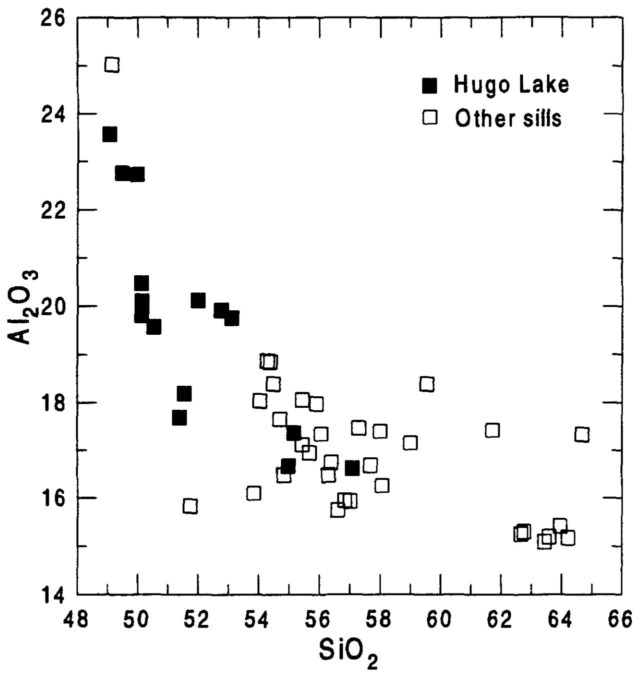


Figure. 13. Plot of $Al_2O_3$ against $SiO_2$ for sills of Hugo Lake and sills and one dike of unit Tai.

The diorite of Pimlico Creek (table 1, no. 39) crops out only along lower Pimlico Creek. It is nearly aphyric, coarse-grained, and hypidiomorphic granular. The body is finer grained near its northern margin, where it has the appearance of a coarse andesite. Anomalous attitudes of volcanic sandstone near the north margin of the intrusion suggest deformation related to intrusion. No contact was observed, but the map pattern shows a clear cross-cutting relation with the wallrock.

## INTRUSIVE SUITE OF KIDD CREEK

Three poorly exposed sills of hornblende dacite and microdiorite crop out in the Hamilton Buttes quadrangle, two in the extreme southwest corner and a thicker one about 1 km west of lower Pimlico Creek. The three sills are petrographically similar to sills and dikes of the intrusive suite of Kidd Creek (Marso and Swanson, 1992), a prominent, voluminous unit that crops out in a 500–km$^2$ area in the East Canyon Ridge, Blue Lake, McCoy Peak, and Tower Rock quadrangles. The one new chemical analysis (table 1, no. 89) from the easternmost body (just south of the quadrangle) is indistinguishable from other analyses of the Kidd Creek suite. Presumably the three sills are coeval with the *ca.* 12–Ma Kidd Creek. Geologic and paleomagnetic evidence indicates that the Kidd Creek magma was emplaced after the older Tertiary rocks were folded (Swanson, 1991, 1992; Hagstrum and Swanson, 1994).

The hornblende microdiorite sill near Pimlico Creek, and its extension just south of the quadrangle, is the easternmost known outcrop of the intrusive suite of Kidd Creek. My unpublished mapping indicates that several sills of the Kidd Creek occur in the northwestern quarter of the Green Mountain quadrangle, but none has been found as far east as that near Pimlico Creek. Still farther east, an extensive cover of Quaternary volcanic rocks could obscure outliers of the Kidd Creek, though there are enough outcrops of Tertiary rocks to make it unlikely that much if any Kidd Creek is hidden.

The Kidd Creek is similar chemically and petrographically to sills and other small bodies of hornblende-bearing quartz diorite and diorite that occur just west of the Cascade Crest a few kilometers northwest and west of White Pass. Ellingson (1959, 1972) collectively assigned these rocks to the Jug Lake pluton. Clayton (1983) showed that these bodies are isolated small intrusions, none of which actually crops out near Jug Lake. Clayton (1983) determined a zircon fission-track age of 11.5 ± 0.4 Ma for one of these intrusions at Laurel Hill; this age is similar to that of the Kidd Creek intrusive suite. These bodies and the Kidd Creek intrusive suite could together be products of a regional pulse of hornblende-bearing dioritic and quartz dioritic magmatism. An additional example of this magmatism could be the youngest part of the Tatoosh Pluton in and just south of Mount Rainier National Park (Wright, 1960; Fiske and others, 1963; Mattinson, 1977; Evarts and others, 1983a).

The Kidd Creek suite is typically lower in $TiO_2$, FeO, and MnO than other Tertiary rocks. This is well shown in plots in my previous open-file reports but only weakly so in figure 14, in which only one Kidd Creek analysis is plotted.

## STRUCTURE

**Folds**—The Pimlico Creek syncline and its right-stepping continuation, the Stonewall Ridge syncline, dominate the structure of the western part of the quadrangle. This domination is reflected by the notable north-northwest mode of strike directions (fig. 12*A*). However, the synclines are poorly defined in places, such as north of Hamilton Buttes and northeast of St. John Lake. Much of the scatter in the rose diagram reflects the gentle north plunge of the broad synclinal troughs.

The synclinal pair defines the next fold east of the Bishop Ridge anticline, whose northwest-trending axial trace is about 7 km farther west (fig. 11). This half-wave-length distance is far less than that between the Bishop Ridge anticline and the Pole Patch syncline some 15 km farther west. In general, wave lengths of folds decrease from west to east across the mapped quadrangles (fig. 11), a pattern recognized farther west too (Evarts and Swanson, 1994).

The Johnson Creek anticline (Winters, 1984) is largely covered by till and Quaternary lava flows. The location of its crest line is well defined near the confluence of Jordan and Johnson Creeks but is uncertain along most of its length. However, the east flank of the fold is reasonably well shown by attitudes along Jordan Creek and on Goat Ridge.

The Johnson Creek anticline brings the arkose of Chambers Creek to the surface. However, an abrupt lithologic change across the crest line suggests a complicated structural or depositional history. West of the crest line, the lower 1–1.5 km of section is mostly arkose. East of the crest, the section is mostly volcanic sandstone and lava flows; arkosic interbeds occur only in the lower few hundred meters.

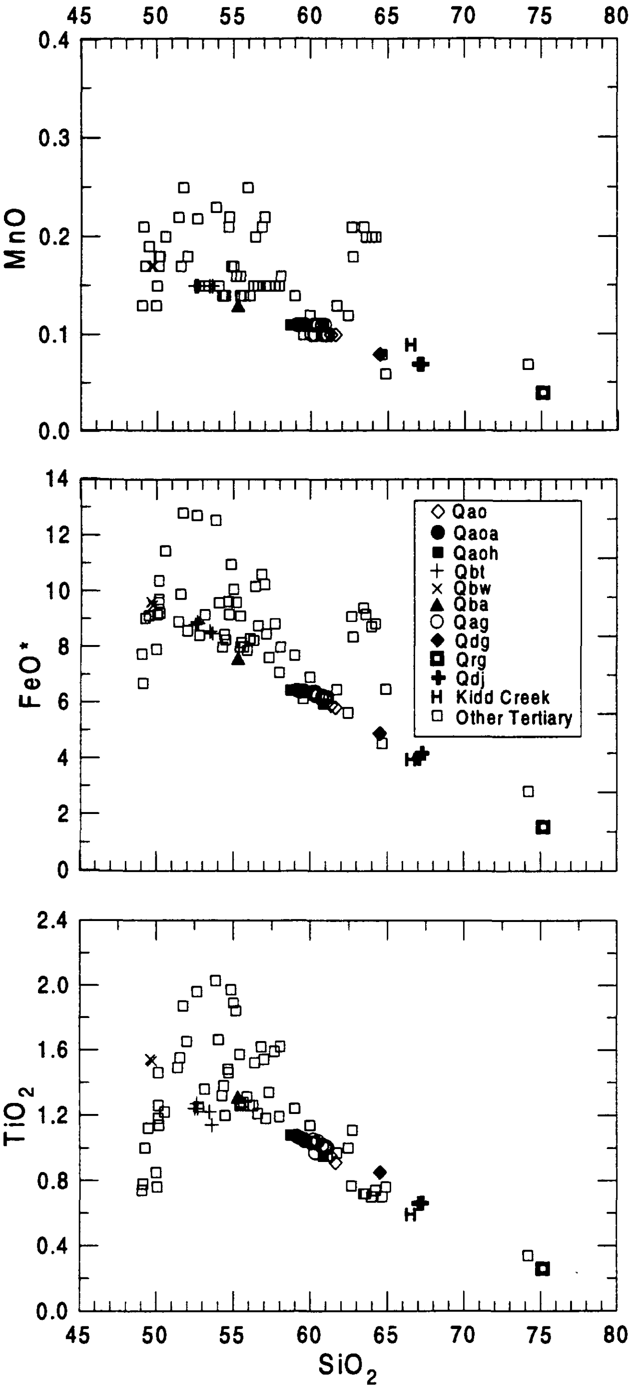


Figure 14. Plots of $TiO_2$, FeO*, and MnO against $SiO_2$ for all analyzed rocks in Hamilton Buttes quadrangle. In other quadrangles, rocks of Kidd Creek intrusive suite are lower in MnO, FeO*, and $TiO_2$ than most other Tertiary rocks. With only one analysis from near this quadrangle, the pattern cannot be seen. See caption of figure 3 for map-unit identifications of Quaternary rocks.

Is this change structurally or depositionally controlled? Exposures are so poor in most critical areas east of the crest line that the answer to that important question may come, if at all, only from study of the Packwood Lake quadrangle, where limited reconnaissance work has been done to date. From the general relations in the Hamilton Buttes quadrangle, the anticline was probably not growing and forming a barrier during deposition, because evidence presented in the section on the arkose of Chambers Creek indicates that the area had to be subsiding to account for the great thickness of the fluvial deposits.

One explanation for the lithologic contrast is that a fault juxtaposes a younger part of the section east of the fault with an older part west of the fault. Map constraints would force the fault to strike roughly north and pass through the Chambers Lake area. It could be a normal fault down to the east, an east-verging reverse or thrust fault, or a strike-slip fault, probably dextral on the basis of regional relations. A wide range in bedding attitudes measured along Jordan Creek might reflect faulting and related drag, although I tentatively prefer an interpretation of modern slumping along the stream bank rather than disruption by faulting.

One difficulty in interpreting the lithologic contrast as controlled by faulting is that the thick section of andesite flows on Goat Ridge has no counterpart on the west limb of the anticline. Andesite flows occur about 400 m stratigraphically higher than arkose on the southwest end of Goat Ridge. In contrast, only volcaniclastic rocks, mostly volcanic sandstone, make up the section for at least 1.5 km above the youngest arkose in the North Fork Cispus drainage (see cross section A–A′ and also Swanson [1993]). Why are there no lava flows or at least coarse debris eroded from them in the drainages of the North Fork Cispus and Mission Creek, if the lithologic contrast is caused by faulting and the east-to-west current directions in the Chambers Creek and younger volcaniclastic rocks are valid? A large strike-slip component seems required if faulting is involved.

**Faults and shear zones**—No major fault was positively identified in the quadrangle, although the preceding discussion of the Johnson Creek anticline points out the possibility of one along or just east of the crest line. No evidence was found to support the northeast-trending faults that Winters (1984) mapped north of Elk Creek and south of Jordan Creek. I interpret his *Hugo Lake lineation*, which bears about 340° through Hugo Lake, to be a strike valley eroded by glaciers, but I can not rule out a fault. From reconnaissance observation, I agree that Winters' northwest-trending, southwest-vergent *Middle Fork reverse fault*, east of Johnson Creek just inside the Packwood Lake quadrangle, *might* be a valid structure, but I haven't completed field work there to test this idea.

Six small faults and related shear zones cut volcanic rocks in the quadrangle. The most obvious is a calcite- and zeolite-rich shear zone cutting lithic-lapilli tuff and volcanic sandstone on the north side of the North Fork Cispus River 1 km downstream from the mouth of Wobbly Creek. The zone is a few tens of centimeters wide and is traceable for almost 1 km from its exposure in a road cut along FS 22. The shear planes strike about 315° and dip about 85° southwest. They commonly have subhorizontal slickensides with a sense of roughness that suggests dextral movement.

Five other small shears were found. All are characterized by narrow zones of broken rock and veins of calcite and (or) zeolite. One of the zones, on Goat Ridge, strikes northwest and has subhorizontal slickensides whose roughness suggests dextral slip. The other four zones strike east-northeast. One is on the ridge north of St. John Creek, another along St. Michael Creek, a third in cuts along FS 78060 1.5 km west-southwest of the mouth of Wobbly Creek, and a fourth in a small creek draining the southeast end of Elk Ridge. All of the east-northeast fault zones have subhorizontal slickensides, but the direction of slip—sinistral—could be determined for only the Elk Ridge shear.

The pattern of north and northwest dextral faults and east and northeast sinistral faults holds throughout all of the mapped quadrangles. It is part of a broad regional pattern well displayed by dextral faults cutting the Columbia River Basalt Group farther southeast, approximately along strike with the mapped area (Walsh and others, 1987).

## PLEISTOCENE LAVA FLOWS AND SUBGLACIAL CONE (TUYA)

Several Pleistocene lava flows occur in the eastern half of the quadrangle. They range in composition from basalt to silicic dacite. Most entered the area from vents farther east, but some were apparently erupted on Goat Ridge. A subglacial vent for basalt lies just east of the southern part of the quadrangle; hyaloclastic debris from the vent crops out within the quadrangle.

**Dacite of Jordan Creek (map unit Qdj)**—This gray to pink, moderately to highly plagioclase-phyric flow caps the ridge north of Jordan Creek, forming a bold cliff visible from near Wright Lake. It occurs mostly in the Packwood Lake quadrangle, where it is extensively covered by till. Outcrops west of the Jordan Creek trail in the Packwood Lake quadrangle indicate that the flow occupies a roughly west-trending valley at least 100 m deep. The flow has a columnar basal zone several meters thick but otherwise is platy, as best seen in the cliff overlooking Jordan Creek.

The flow contains several generations of large plagioclase phenocrysts and glomerocrysts (including dusty and rounded crystals and clots), phenocrysts of two pyroxenes and rare hornblende, and uncommon xenocrysts of quartz in a blotchy, cryptocrystalline groundmass. Crystalline clots 1–2 cm in diameter of plagioclase and two pyroxenes are common and readily seen in the field. Oxidized crystals of hypersthene give hand samples a dark spotted appearance. The rock is a silicic dacite with 67.1–67.3 percent $SiO_2$ (table 1, nos. 90–91).

I interpret the dacite of Jordan Creek to be a down-valley erosional outlier of a thick sequence of andesite and dacite flows erupted from Goat Rocks volcano (Ellingson, 1968; Swanson and Clayton, 1983; Church and others, 1983). One of these flows moved westward down the ancestral valley of Jordan Creek–Middle Fork Johnson Creek (about 3 km north of Jordan Creek), which is radial to the volcano. Later incision into or along the side of the flow carved the modern canyons of Jordan and Middle Fork Johnson Creeks.

The dacite has a second possible source, though I think that source is unlikely on geomorphic grounds alone. The flow could have been erupted from a vent on Goat Ridge and flowed northwest across a shallow ancestral valley of Jordan Creek, spilling over the ridge north of the creek and moving into the drainage of Middle Fork Johnson Creek.

Both hypotheses share the same weakness. The dacite is chemically unlike any flow that I have found either up Jordan Creek or on Goat Ridge (table 1; my unpublished chemical analyses). The dacite is more silicic than most other flows in these two areas and does not physically resemble the still more silicic rhyolite of Goat Ridge (map unit Qrg). I have not sampled all flows up Jordan Creek but have probably sampled all on Goat Ridge. This is another reason that I favor a source up Jordan Creek at Goat Rocks volcano. Moreover, typical flows from the volcano are far more voluminous than those erupted on Goat Ridge, so it would have been more likely for such flows to have advanced far away from the source. But, both the dacite of Jordan Creek and the dacite of Goat Ridge have relatively high contents of $K_2O$ (fig. 10) and could be products of related magmas.

The age of the dacite of Jordan Creek is poorly known. Till of Evans Creek Drift overlies the dacite just north of the quadrangle. I recognized no remnants of the older Hayden Creek Drift, possibly because of erosion during Evans Creek time. The flow has normal magnetic polarity and so is most likely either younger than 0.78 Ma or older than about 1.76–1.77 Ma (Cande and Kent, 1992, 1995; Izett and Obradovich, 1994; Berggren and others, 1995). Most of the flows farther up Jordan Creek are magnetically reversed and probably were erupted during the Matuyama Chron (0.77–1.75 Ma); only the youngest has normal polarity (D.A. Swanson, unpublished data, 1982 and 1995). The dacite of Jordan Creek seems to occupy a valley that farther upstream is eroded into the reversed flows; if so, it is most likely younger than about 0.78 Ma (Brunhes Chron), although it could be about 0.92–1.11 Ma (Jaramillo Normal Subchron; Izett and Obradovich, 1994; age is 0.99–1.07 Ma according to Berggren and others [1995]) or 1.21–1.24 Ma (Cobb Mountain Normal Subchron; Berggren and others, 1995). Its high degree of erosion suggests an early Brunhes or older age.

**Andesite, dacite, and rhyolite of Goat Ridge**—Several sparsely to moderately but finely porphyritic lava flows of pyroxene andesite (map unit Qag; table 1, nos. 62–70, 72–75) cap the southwest end of Goat Ridge and spill northward toward Jordan Creek valley and southward into Goat and Chambers Creek valleys. The flows typically contain small phenocrysts and microphenocrysts of plagioclase and two pyroxenes with or without sparse, small oxidized needles of hornblende. The phenocrysts and microphenocrysts are commonly flow-aligned. Typically the groundmass consists of blocky, flow-aligned plagioclase microlites in a glassy or cryptocrystalline matrix. Most flows are quite platy as a result of the aligned microlites,. Subspheroidal lithic inclusions of intergrown plagioclase and two pyroxenes, probably cognate clots, are ubiquitous and locally are several centimeters in diameter. Such inclusions are abundant at the end of the longest flow along Chambers Creek (table 1, no. 73; Stop 3-10 in Evarts and Swanson [1994], who assigned the flow to the andesite of Old Snowy Mountain). This particular flow lacks microphenocrysts of clinopyroxene, but other flows of the unit carry both pyroxenes.

The vent(s) for the andesite of Goat Ridge must have been on the crest of Goat Ridge, because lava moved down both flanks of the ridge. However, no remnant of a cone remains, apparently owing to glacial erosion. Oxidized, rubbly andesite on the west side of Point 6201 might be near-vent material but is more likely part of a rubbly flow. The lack of definite vent deposits on Goat Ridge led me to consider that the andesite might be down-valley remnants of flows erupted from Goat Rocks volcano. However, the elevation of the flows and the intervening topography make this interpretation untenable.

Scattered, discontinuous outcrops of andesite whose platy jointing consistently dips downslope, combined with a locally thick mantle of till, cause the lower southeast side of Goat Ridge to resemble a large landslide. However, field readings with a fluxgate magnetometer on andesite in isolated outcrops and trail cuts gave consistent orientations and strong normal polarity. No evidence for block rotation was found, except in talus and in the one mapped landslide, which has obvious geomorphic expression where the foot trail crosses it.

The isolated patch of andesite 1.5 km north-northwest of Chambers Lake is somewhat different from the rest of the unit, for it contains 2–3 percent of hornblende phenocrysts as long as 2 mm. Hornblende in most of the unit is generally less abundant and smaller. Otherwise, the flow resembles the other andesite flows on Goat Ridge—finely and sparsely plagioclase phyric, platy, fine-grained, and 15–20 m thick.

At least one flow of magnetically normal mafic dacite (map unit Qdg) occurs on Goat Ridge and was probably erupted from the same area that produced the andesite (table 1, nos. 86). This flow was recognized only on the north flank of the ridge but might be present elsewhere beneath till or younger andesite. In general the dacite resembles the andesite on Goat Ridge but is lighter gray than most, has a glassier, "sugary"(under the hand lens) groundmass, and contains several percent of plagioclase phenocrysts as long as 5 mm. Each examined thin section contains a rounded quartz xenocryst and at least one large phenocryst of dusty plagioclase. The rock looks mixed and physically resembles the dacite of Jordan Creek though less silicic and somewhat less porphyritic. It is probably 50–60 m thick and may have ponded in ancestral Jordan Creek valley.

A light-colored, intricately flow-layered rhyolite flow (rhyolite of Goat Ridge, map unit Qrg) crops out along a small creek 2.5 km north-northwest of Chambers Lake. The rock is fresh and has a $SiO_2$ content of about 75 percent (table 1, no. 93; note the low LOI of only 0.25 wt percent). It has an exceptionally high $K_2O$ content (fig. 10) of more than 4 percent. The rhyolite contains sparse, small plagioclase and orthopyroxene phenocrysts and rare olivine xenocrysts(?), and has a streaky, blotchy, cryptocrystalline groundmass. The rhyolite lacks cognate lithic inclusions, which are present in all other flows on Goat Ridge (and in most flows from Goat Rocks volcano, too). It rests directly on volcanic sandstone but is otherwise surrounded by till. Its magnetic polarity was not determined. The freshness of the rock suggests a Pleistocene age, and it may have a source on Goat Ridge, perhaps as a precursor to the dacite. This rock is one of the most silicic yet analyzed in the Quaternary Cascades of Washington.

The andesite of Goat Ridge flowed into and then along the ancestral Chambers Creek-Goat Creek valley after this valley had nearly reached its present elevation. Consequently the andesite is most likely younger than the Hayden Creek Drift, about 0.14 Ma. However, this evidence is not compelling, and the andesite could be older than the Hayden Creek though probably younger than 0.77 Ma, because of its consistently normal magnetic polarity.

In the Chambers Creek-Goat Creek valley, the andesite of Goat Ridge is distinguished in the field from the younger, nearly aphyric andesite of Old Snowy Mountain by its greater number and size of phenocrysts. However, this criterion is difficult to apply, for the Goat Ridge rocks themselves are not strongly porphyritic. In many places along the valley, flows or parts of flows contain few phenocrysts, and it becomes very difficult to assign with confidence a particular outcrop to one of the units. Thin sections show that the groundmass microlites in the Goat Ridge flows are typically larger and more widely spaced throughout the matrix than in the Old Snowy Mountain flows, which have pilotaxitic texture. It took me a long time (and the collection of twelve additional samples in June 1995) to arrive at the current map presentation, which depends largely on thin-section identification combined with geomorphic evidence. Dotted contacts on the map portray where I think the present contact between the two andesitic units lies under till.

Chemical composition is no aid in distinguishing the andesite of Goat Ridge from the andesite of Old Snowy Mountain. All of the plots show a tight cluster of analyses for both units (figs. 3, 8–10, and 14).

An especially tenuous assignment involves the flow forming an arcuate ridge 10–12 m high 1 km northwest of the confluence of Goat Creek and Cispus River. This flow is glassy to very fine-grained and almost non-porphyritic. Welded or agglutinated breccia, some oxidized and well-sorted, is common in middle parts of the flow. The few phenocrysts and glomerocrysts are orthopyroxene and clinopyroxene, less than 1 mm across; no plagioclase phenocrysts are found. In this respect the flow is petrographically unlike either the Goat Ridge or Old Snowy Mountain andesite. It is remarkable for its local concentrations of fresh lithic inclusions, almost certainly cognate. Hand samples from some parts of the flow consist mostly of inclusions. I tentatively include the andesite in the Goat Ridge unit only because it forms a ridge that reasonably is an erosional remnant around which advanced the younger andesite flows of Old Snowy Mountain. However, the ridge could be the remains of an isolated vent, as suggested by its height and arcuate shape (concave southward), the abundance of welded or agglutinated breccia (airfall?), and the concentrations of inclusions (near-vent lag?). Chemically (table 1, no. 56), the flow resembles both the other andesite of Goat Ridge and the aphyric andesite of Old Snowy Mountain (map unit Qaoa). Possibly the ridge represents the vent for unit Qaoa, which has not been found farther upstream, although the flow in the ridge contains more phenocrysts and lithic inclusions than does unit Qaoa.

**Andesite of Old Snowy Mountain**—These flows, first recognized and named by Ellingson (1968), were erupted from glacially destroyed vents in the Old Snowy Mountain–Ives Peak area in the Goat Rocks volcanic center, about 5 km northeast of the map area. The flows entered the upper drainages of the Cispus River and Goat Creek and moved downstream, converging 1–2 km east of the map area before advancing several kilometers farther southwest. The result is the broad valley fill so prominent along lower Goat Creek and adjacent Cispus River. The higher parts of the andesite unit underlie the alpine meadows of Snowgrass Flat, the most heavily visited part of the Goat Rocks Wilderness, 3 km east of the quadrangle.

The flows are very fine grained and pilotaxitic, with abundant glass. The pilotaxitic texture is striking and of textbook quality; numerous small shear planes, defined by changes in microlite orientation, are present in each thin section. The flows are either aphyric or more commonly contain very few small phenocrysts or microphenocrysts of plagioclase and (or) hornblende (an exception is the hornblende-phyric andesite of unit Qaoh). All are highly platy and several to several tens of meters thick. Most contain cognate lithic inclusions, but the aphryic flows do not. The flows can be separated into three units on the basis of their petrographic character, identifiable both in the field and in thin section. Age relations among the three units are problematic, however, and the petrographic units might even intertongue rather than having distinctly different ages. Detailed work in the Walupt Lake and Old Snowy Mountain quadrangles, where the Evans Creek Drift is not as thick and erosional relief is greater, may help to clarify the age relations.

The most extensive flows (unit Qao) contain a few small phenocrysts or microphenocrysts of plagioclase, two pyroxenes, and hornblende in descending order of abundance. Lithic inclusions are abundant. The two available chemical analyses are similar and andesitic (table 1, nos. 76 and 77), with a marginally higher $SiO_2$ content than the andesite of Goat Ridge but otherwise similar. The flows of unit Qao closely resemble those near and on Old Snowy Mountain (though about 1 percent richer in $SiO_2$), and the plug at Ives Peak could be a coarser variety (though about 2 percent poorer in $SiO_2$), to judge from my unpublished observations and chemical analyses of the Old Snowy Mountain-Ives Peak area.

A unit (Qaoa) of one or more thick (60 m or more) aphyric to very sparsely two pyroxene-plagioclase-phyric flows follows the Cispus River along the eastern edge of the quadrangle (table 1, nos. 55 and 59). It is well exposed in a large roadside quarry at its southern terminus (table 1, no. 58; Stop 3-11 of Evarts and Swanson, 1994), where its uniformly aphyric texture is striking. A similar, perhaps the same, flow follows the Cispus River just inside the Walupt Lake quadrangle and underlies the spectacular falls and cascades at the mouth of Walupt Creek. The aphryic unit may have followed the Cispus along a canyon eroded into earlier flows of unit Qao, although no definitive age relations between the two units were found. The flows are sensibly nonporphyritic but locally contain tiny red-brown oxidized microphenocrysts of hypersthene or hornblende and rare olivine.

The third unit (Qaoh) contains several percent of phenocrysts of oxyhornblende, generally about 1 mm long but as long as 3 mm. Accompanying the hornblende are phenocrysts and microphenocrysts of plagioclase and, in some flows, hypersthene. These flows do not extend far into the quadrangle and can be reached only by foot, most conveniently from the trail to Snowgrass Flat. The unit near the confluence of Goat Creek and Cispus River contains fewer hornblende phenocrysts and is more mafic (table 1, no. 53) than flows farther upstream (table 1, no. 71). A flow of unit Qao appears to overlie a flow of unit Qaoh at one place along Goat Creek just south of the trail about 0.5 km inside the Walupt Lake quadrangle; however, talus obscures the contact, and the hornblende-phyric flow could occupy a gorge eroded into an older flow of unit Qao. Hornblende-phyric flows form cliffs shedding abundant talus along the north side of the Cispus River for 3 km (by river) east of the mapped area. A hornblende-phyric flow possibly belonging to the unit crops out at 4000 ft elevation 0.5 km northwest of Walupt Lake Campground, 2 km east of river mile 47 on the Cispus River; a thick flow of unit Qaoa occupies a gorge along the Cispus eroded through this hornblende-phyric flow.

The andesite of Old Snowy Mountain is younger than the andesite of Goat Ridge, for it occupies the Goat Creek-Cispus River valley, which has been eroded into the Goat Ridge flows. It comprises the youngest flows of Goat Rocks volcanic center. The flows were erupted after a pause (probably several hundred thousand years) in volcanism that allowed time for incision of deep canyons into the pyroxene andesite flows that form most of Goat Rocks volcano, a late Pliocene(?) to middle Pleistocene edifice now largely eroded away (Ellingson, 1968; Swanson and Clayton, 1983; Clayton, 1983; Church and others, 1983). The vents for the young andesite are apparently in the Old Snowy Mountain–Ives Peak area, 3–4 km southeast of the center of Goat Rocks volcano as defined by the focus of a radial dike swarm (Swanson and Clayton, 1983; Church and others, 1983). Whether the vents are on Old Snowy Mountain and Ives Peak themselves (Swanson and Clayton, 1983) or were located just east of there before removal by glaciation (Ellingson, 1968) is uncertain.

The andesite of Old Snowy Mountain has been identified along the Cascade crest at the supposed vents on Old Snowy Mountain and Ives Peak, and in lava flows west of the crest along Goat Creek, upper Cispus River, and Upper Lake Creek (in the Old Snowy Mountain and Packwood Lake quadrangles; Ellingson, 1968; Swanson and Clayton, 1983; Church and others, 1983). All flows have normal magnetic polarity and so are almost certainly younger than about 0.77 Ma. The flows followed drainages similar to those of today in both width and depth, and they are overlain only by till of the Evans Creek Drift, about 20 ka. Probably, therefore, they postdate the Hayden Creek Drift (0.14 Ma), as also interpreted by Ellingson (1968), and should overlie it somewhere. However, no exposures of the base of the unit have yet been found in areas where the Hayden Creek Drift might be expected to be present.

**Basalt and basaltic andesite in southeastern corner of quadrangle**—At least two lava flows and part of one subglacial volcano crop out in this poorly exposed area. All three map units have normal magnetic polarity but have been glaciated and so are probably late Pleistocene.

***Basalt of Walupt Lake volcano (map unit Qbw)***— Road cuts along FS 2164 expose hyaloclastic deposits of bedded, well sorted to poorly sorted sideromelane sand containing blocks of glassy olivine-bearing basalt. The beds dip downslope but are commonly irregular and lensoid.

I interpret these deposits as part of Walupt Lake volcano (Hammond, 1980; Swanson and Clayton, 1983; Church and others, 1983), a mostly subglacial edifice centered 2– 2.5 km east of the road cuts. The volcano stands more than 500 m above its north base. It is composed dominantly of hyaloclastic debris. However, its upper 60–90 m is made of subhorizontal flows of olivine basalt capped by a few meters of oxidized bedded cinder; this part of the edifice formed when the volcano grew above the surface of the glacier. The subaerial flows give a flat-topped appearance to the volcano, creating a tuya. The road cuts show only a small part of the variety of deposits in the cone.

Chemical analyses were obtained on two samples of the basalt of Walupt Lake volcano from just inside the Walupt Lake quadrangle yet more than 1 km apart (table 1, nos. 5 and 6). The analyses are very similar and significantly more mafic than those of the adjacent basalt of Two Lakes (table 1, nos. 18–20, 24, and 25).

Hammond (1980) considered Walupt Lake volcano to have formed within the Evans Creek ice sheet. However, the aphyric andesite flow of Old Snowy Mountain (unit Qaoa) abuts and wraps around the base of the volcano and is not overlain by basaltic hyaloclastic debris from it. The andesite flow underlies Evans Creek Drift and therefore predates the time that the Evans Creek glacier advanced this far down the valley. I think it probable that Walupt Lake volcano formed during a previous glaciation, probably about 0.14 Ma during the time of Hayden Creek glaciation.

***Basalt of Two Lakes (map unit Qbt)***—The basalt of Two Lakes probably underlies much of the till-mantled slope south of Walupt Lake volcano and east of the Cispus valley. The unit was named by Hammond (1980) for exposures on the Yakama Indian Reservation in the Two Lakes area, 3 km east of the southeast corner of the quadrangle.

Several flows, each a few meters thick, form the basalt of Two Lakes. They typically contain a few percent of olivine phenocrysts and small plagioclase phenocrysts. The unit cannot be readily distinguished from the more mafic basalt of Walupt Lake volcano by its phenocryst population, though it may on average contain more and larger olivine phenocrysts. Consistent with its subaerial nature, the unit generally has a more crystalline, intergranular texture than the quenched Walupt Lake basalt. Chemically, the unit is mafic basaltic andesite (table 1, nos. 18–19, 21, and 24–25), which cannot be distinguished from basalt in the field. Several possible vent areas have been recognized in the Walupt Lake quadrangle, though only small remnants of cinder deposits survived the Evans Creek glaciation.

One kilometer north of the Lewis County line, a basalt flow (table 1, no. 25) forms a flat bench bounded by a west-facing cliff 20 m high.. This flow may be a remnant of one that entered the valley while thin ice remained or before outwash deposits were removed down to their present elevation.

At least some of the basalt of Two Lakes is younger than the basalt of Walupt Lake volcano, because flows moved around the south base of the volcano and lack a cover of hyaloclastic debris. The flow at the site of chemical analysis 18 is olivine-plagioclase-microphyric basalt that is blockly jointed, has pillow-like masses, and is clearly quenched. So, at least some of the basalt of Two Lakes probably interacted with ice or meltwater.

***Basaltic andesite (map unit Qba)***—A flow of moderately olivine-clinopyroxene-plagioclase-phyric basaltic andesite (table 1, no. 36) forms a 35–m–high, flat-topped cliff overlooking the Cispus valley below the road cuts through Walupt Lake volcano. The flow is intersertal and may be somewhat quenched. It has several percent of plagioclase phenocrysts, generally riddled with glass inclusions, as large as 4 mm in diameter. These large and fairly numerous phenocrysts distinguish the flow from other olivine-bearing basalt in the area. The bench-like morphology of the outcrop, similar to that of the Two Lakes flow described above, suggests an erosional remnant of a flow that once filled part of the Cispus valley, perhaps while ice or outwash deposits occupied the valley. Probably the flow was erupted from an unidentified vent in the Walupt Lake quadrangle just south of Walupt Lake volcano, where there is an extensive area of late Pleistocene basalt and basaltic andesite. The age of the flow relative to Walupt Lake volcano and the basalt of Two Lakes is not known; most likely it is older, because it crops out nowhere else and may be buried by younger deposits or have been eroded away.

## QUATERNARY SEDIMENTARY DEPOSITS

**Glacial deposits**—Till mantles most of the eastern part of the quadrangle. Small ponds and marshes commonly dot the deposits. Fine-grained andesite clasts in the till have slight if any weathering rinds, so the till almost surely correlates with the Evans Creek Drift (map unit Qed; Colman and Pierce, 1981; Crandell and Miller, 1974). This identification is particularly good in and along the Cispus River and Goat and

Chambers Creeks, where Quaternary andesite constitutes most of the stones.

Correlation of till with Evans Creek Drift is less certain in the valleys of the North Fork Cispus River and Pimlico and Wobbly Creeks, because the Tertiary bedrock contains little competent, fine-grained andesite such as that generally used to evaluate weathering-rind thickness (Colman and Pierce, 1981). Some or all of the till and other surficial deposits in these drainages could be Hayden Creek Drift, and some could be colluvium or old landslide material.

Most lakes in the quadrangle owe their origin to glaciation associated with the Evans Creek Drift. Chambers Lake and the marsh extending farther northwest occupy depressions on a glaciated divide; the marsh is probably entirely within till, but Chambers Lake may be floored by bedrock. Mud Lake northwest of Hamilton Buttes lies in a similar setting, in till on the divide between Timonium and Wobbly Creeks. Hugo Lake and the marshy flat farther north are also in till on the divide at the head of Johnson Creek. St. Michael and St. John Lakes, near the northwestern edge of the quadrangle, both rest in small cirques surrounded by bedrock. Presumably these lakes all postdate Evans Creek Drift.

Thick deposits mainly of andesitic gravel (map unit Qgs) border the floodplain of the Cispus River where it widens downstream beyond the andesite of Old Snowy Mountain. The gravel is probably outwash of Evans Creek Drift carried by the Cispus as the valley glacier receded into the Goat Rocks high country. I interpret the gravel to correlate with outwash farther downstream in the East Canyon Ridge quadrangle (Swanson, 1994). There, however, the unit consists dominantly of *basaltic* gravel derived from Late Pleistocene flows north of Mount Adams (Hildreth and Fierstein, 1995; Hildreth and Lanphere, 1994). Apparently the flood of basaltic gravel from this area greatly diluted the andesitic gravel coming from farther upstream.

**Landslide deposits (map unit Qls)**—Landslides are common through the quadrangle. They are particularly large on steep dip slopes in Tertiary rocks. Three slides or slide complexes are especially noteworthy.

Wobbly Lake is dammed by the youngest in a complex of landslides that peeled away from steeply west-dipping, bedded volcaniclastic rocks (mostly volcanic sandstone and siltstone) on the west side of Elk Ridge. The Wobbly Lake slide started about 1 km south of Elk Peak, advanced into and down a northwest-flowing tributary of Wobbly Creek, crossed the creek, and rode up on the west wall of the valley more than 60 m before coming to a halt. The slide crossed at least two older landslides, as indicated by the dashed contacts on the geologic map. Deep closed depressions dot the surface of the slide, which probably is no older than a few thousand years. Wobbly Creek now enters the lake as a surface flow but drains the lake underground to a point about 850 m downstream, where the water emerges in springs from the rocky toe of the landslide deposit.

The west side of Elk Ridge is essentially a dip slope, and blocks of volcanic sandstone locally dot the slope as if they had glided into place along slippery beds. Such areas are not portrayed as landslides on the map, but clearly the entire slope is potentially susceptible to block gliding or landsliding during a large earthquake. Possibly the large slide that formed Wobbly Lake had just such a trigger.

A rockfall-landslide deposit 2 km north of Hugo Lake heads in a steeply west-dipping microdiorite sill intruded into arkose and volcanic sandstone. It moved to the floor of Johnson Creek, where its rocky margin is prominent in an open, locally marshy meadow just east of FS 21. Hand-augering by Pat Pringle (Washington Division of Geology and Earth Resources), Bob Schuster (U.S. Geological Survey), and me on the landslide deposit near the meadow found probable $W_e$ tephra from Mount St. Helens, erupted in 1482 AD (Yamaguchi, 1985).

A landslide from the steep west flank of Johnson Creek valley cascaded into and then along the creek for about 1 km, nearly reaching the northern edge of the mapped area. Wright Lake, shown though unnamed on the quadrangle, occupies a broad depression on the slide deposit. This slide heads in a west-dipping section of arkose—an exception to the generality that the large slides move down dip.

Elsewhere in the quadrangle the distinction between landslide and colluvial deposits is often difficult to make, particularly on forested slopes. Much of the colluvium mapped as unit Qc could contain landslide debris.

# DESCRIPTION OF MAP UNITS

## SURFICIAL DEPOSITS

**Qal** **Alluvium (Holocene and Pleistocene)**—Unconsolidated, moderately to well-sorted deposits of silt, sand, and gravel along major modern streams and in small basins. Mostly Holocene and very late Pleistocene. Locally includes colluvium, fan deposits, and drift

**Qc** **Colluvium (Holocene and Pleistocene)**—Unsorted, unconsolidated deposits of slope wash and open-work talus, mostly along sides of major streams and below cliffs. Mostly Holocene and very late Pleistocene. Locally includes alluvium, landslide deposits, fan deposits, and drift

**Qf** **Alluvial fan deposits (Holocene or Pleistocene)**—Poorly bedded and sorted alluvial deposits, in part debris flows, at mouths of two small tributaries of North Fork Cispus River. Holocene or very late Pleistocene. May include alluvium, colluvium, and drift

**Qls** **Landslide deposits (Holocene and Pleistocene)**—Diamictons produced by mass movement down slope. Includes both active and inactive slides. Wobbly and Wright Lakes both result from landslides. Most record failure on steep dip slopes. Some slides result from movement of relatively dense microdiorite or andesite across volcaniclastic rocks. Others developed wholly in volcanic sandstone and related deposits. Mostly Holocene and very late Pleistocene. Locally includes colluvium and drift

## GLACIAL DEPOSITS

**Qed** **Evans Creek Drift (Pleistocene)**—Till and outwash deposits, principally along Cispus River. Slightly weathered to unweathered; most clasts in B soil horizon lack significant weathering rinds. Age is late Pleistocene, approximately 17–25 ka (Barnosky, 1984; Crandell, 1987). Queried where possibly of Hayden Creek age along North Fork Cispus River. Locally divided into:

**Qgs** **Gravel and sand deposits (Pleistocene)**—Poorly to well-sorted, subangular to rounded fluvial gravel and sand in the Cispus River valley. Includes diamictons, probably deposited by debris flows. Thought to represent outwash from melting ice in Cispus drainage. Probably the upstream, less well-sorted and rounded equivalent of outwash deposits mapped in Blue Lake, Tower Rock, and Greenhorn Buttes quadrangles. Overlies late Pleistocene basalt of Spring Creek in East Canyon Ridge quadrangle. Locally includes alluvium

**Qhd** **Hayden Creek Drift (Pleistocene)**—Possible till along North Fork Cispus River. Contains clasts with weathering rinds 1–2 mm thick in B soil horizon. Such rinds suggest correlation with Hayden Creek Drift (Crandell and Miller, 1974; Colman and Pierce, 1981). Identification is tentative, owing to uncertainties in distinguishing till from old landslide or colluvial deposits, or especially from younger Evans Creek Drift. Age late Pleistocene but otherwise uncertain; estimates range from about 60 ka (Crandell and Miller, 1974; Crandell, 1987) to 300 ka (Dethier, 1988). Colman and Pierce (1981) prefer age of about 140 ka on basis of thickness of weathering rinds. May include alluvium, colluvium, and younger drift

## YOUNG LAVA FLOWS AND RELATED DEPOSITS

**Qdj** **Dacite of Jordan Creek (Pleistocene)**—Gray to pink dacite flow, moderately to highly pyroxene-plagioclase-phyric, capping ridge north of Jordan Creek. About 60 m thick. Columnar basal zone several meters thick but otherwise platy. Contains crystalline clots of plagioclase and two pyroxenes 1–2 mm in diameter. Xenocrysts of quartz. Chemically a dacite with about 67 percent $SiO_2$ (table 1, nos. 90–91) Probably an intracanyon flow erupted from Goat Rocks volcano. Normal magnetic polarity. Covered with Evans Creek Drift north of quadrangle

**Qao** **Andesite of Old Snowy Mountain (Pleistocene)**—Light gray, sparsely and finely hornblende-two pyroxene-plagioclase-phyric andesite flows erupted from Old Snowy Mountain–Ives Peak area 5 km northeast of map area. Typically fine-grained and pilotaxitic. Lithic inclusions (intergrowths of plagioclase and one or two pyroxenes), generally subspheroidal and less than 3 cm in diameter, are common. Silicic andesite with about 61 percent SiO2 (table 1, nos. 76–77). Occupies modern valley of Goat Creek and upper Cispus River and so probably younger than Hayden Creek Drift. Normal magnetic polarity. Locally divided into:

**Qaoa** **Nonporphyritic andesite of Old Snowy Mountain**—One or more nonporphyritic to very sparsely and finely porphyritic, platy andesite flows, 60 m or more thick, exposed along Cispus River on east edge of map area. Some samples contain a few tiny microphenocrysts of oxidized hypersthene or hornblende and rare olivine. Free of lithic inclusions. Andesitic composition (table 1, nos. 55 and 58–59)

**Qaoh** **Oxyhornblende andesite of Old Snowy Mountain**—Andesite flows containing several percent of small oxyhornblende and plagioclase phenocrysts. Hornblende commonly hard to recognize in the field, because of its size and oxidized nature. Occurs in quadrangle only near confluence of Goat Creek and Cispus River but is prominent farther east. Andesitic composition (table 1, nos. 53 and 71)

**Qag** **Andesite of Goat Ridge (Pleistocene)**—Sparsely to moderately but finely two-pyroxene-plagioclase andesite on south end of Goat Ridge. Some flows carry small needles of oxidized hornblende, and flow 1.5 km north-northwest of Chambers Lake contains 2–3 percent hornblende phenocrysts as long as 2 mm. Typically has pilotaxitic groundmass, with microlites commonly flow aligned; prominent platy jointing results from this texture. Ubiquitous lithic inclusions of plagioclase and two pyroxenes. Silicic andesite chemically (table 1, nos. 62–70, 72–75, and possibly 56). Erupted from crest of Goat Ridge, but glaciation has removed all trace of cones. Normal magnetic polarity. Underlies Evans Creek Drift. Locally subdivided into:

**Qdg** **Dacite of Goat Ridge**—Mafic dacite (table 1, no. 86), similar in appearance to andesite of Goat Ridge but is lighter gray, has glassy groundmass, and contains several percent plagioclase phenocrysts as long as 5 mm. Scattered phenocrysts of dusty plagioclase and resorbed xenocrysts of quartz. Found only on northwest flank of Goat Ridge

**Qrg** **Rhyolite of Goat Ridge**—Fresh, intricately flow-layered, sparsely plagioclase and orthopyroxene-phyric rhyolite (table 1, no. 93) 2.5 km north-northeast of Chambers Lake. Magnetic polarity not determined. Older than at least one flow of unit Qag, but probably of Pleistocene age

**Qbt** **Basalt of Two Lakes of Hammond (1960) (Pleistocene)**—Several flows of slightly olivine-plagioclase-phyric basaltic andesite in southeastern part of map area. The basaltic andesite is mafic (table 1, nos. 18–19, 21, and 24–25) and closely resembles basalt in hand sample and thin section. Normal magnetic polarity. Erupted from vents just east of mapped area. Petrographically resembles basalt of Walupt Lake volcano. Underlies Evans Creek Drift; some flows could predate Hayden Creek Drift. In part younger than Walupt Lake volcano

**Qba** **Basaltic andesite (Pleistocene)**—Flow of moderately olivine-clinopyroxene-plagioclase-phyric basaltic andesite (table 1, no. 36) forming 3–5-m-high bench overlooking Cispus valley in southwestern part of mapped area. Intersertal texture. Probably remnant of intravalley flow, but source unknown

**Qbw** **Basalt of Walupt Lake volcano (Pleistocene)**—In mapped area, consists mostly of hyaloclastic deposits of bedded sideromelane sand containing blocks of glassy olivine-bearing basalt. Hackly jointed, pillow-like masses of quenched basalt also present. Two chemical analyses closely resemble one another (table 1, nos. 5–6). Forms small part of large subglacial volcano, first recognized by Hammond (1980), in adjacent Walupt Lake quadrangle (Swanson and Clayton, 1983). Probably formed beneath valley glacier during Hayden Creek time

## INTRUSIVE ROCKS

**Thd** **Hornblende microdiorite and dacite (Miocene)**—Hornblende-clinopyroxene-plagioclase-phyric microdiorite and dacite forming three sills in southwestern corner of quadrangle. Similar rocks occur farther west for some distance and form the comagmatic *intrusive suite of Kidd Creek* of Marso and Swanson (1992). Grain size largely depends on thickness of body: dacite in thin sills and chilled margins of larger bodies, and microdiorite (fine-grained diorite) in thick sills. Average grain size typically is 0.2–0.4 mm. Hornblende occurs in groundmass but chiefly as phenocrysts as long as 5 mm, with scattered megacrysts and clots to more than 1 cm in diameter. Hornblende phenocrysts form 1–5 percent of rock, clinopyroxene phenocrysts 1– 3 percent, and plagioclase phenocrysts, about 5– 15 (rarely 20) percent. Sparse orthopyroxene present in some samples. Groundmass quartz present in some microdiorite. Inclusions of variously textured diorite, and clots of hornblende and plagioclase, fairly common. Unit is chemically dacite (table 1, no. 89), slightly richer in $SiO_2$ than most of unit elsewhere but within the overall range. Relatively low $TiO_2$, FeO*, and MnO compared to host rocks at similar $SiO_2$ content. Generally fresher than host rock; hornblende is commonly unaltered. Age is about 12 Ma on basis of three zircon fission-track ages outside the quadrangle (Swanson, 1991, tables 2 and 3)

**Taim** **Basaltic andesite intrusion south of St. Michael Lake (Miocene or Oligocene)**—Highly jointed, fine- to medium-grained, nonporphyritic to seriate (plagioclase and clinopyroxene) intrusion. Nearly vertical contact with host rock exposed along western and northern margin of body in adjacent Blue Lake quadrangle. Typically forms craggy outcrops. Basaltic andesite composition (Swanson, 1993, table 1, nos. 24 and 25). Zeolites locally abundant

**Tdip** **Diorite of Pimlico Creek (Miocene and Oligocene)**—Nearly aphyric, coarse-grained, hypidiomorphic granular diorite or gabbro cropping out only along lower Pimlico Creek. Coarse andesite along northern margin, where adjacent wallrock is deformed. Basaltic andesite composition (table 1, no. 39). No contact observed, but map pattern shows clear cross-cutting relation with the wallrock

**Taih** **Sills of Hugo Lake (Miocene and Oligocene)**—Highly and generally coarsely plagioclase-phyric basalt, basaltic andesite, and lesser diabase and microdiorite forming numerous sills cutting arkose of Chambers Creek and younger volcaniclastic rocks. Typically columnar jointed and 4–7 m thick. Commonly forms strike ridges 2 km or more long. Plagioclase phenocrysts 3–6 mm long, and a few glomerocrysts as much as 10 mm or more across, form 10–30 volume per cent of rock. Phenocrysts of pyroxene (both hypersthene and augite) generally make up a few per cent. From glassy (now devitrified) or very fine-grained margins, grain size increases toward interior, reaching 1–2 mm in coarsest microdiorite. Chemical analyses range from basaltic (table 1, nos. 1, 4, 7, 9–11, and 14–15) to basaltic andesite (table 1, nos. 17, 22–23, and 34–35) to mafic andesite (table 1, no. 48). The more mafic rocks commonly have high contents of $Al_2O_3$ and CaO, suggestive of plagioclase accumulation. Several dikes of unit Tai are highly plagioclase porphyritic and are likely related to sills of Hugo Lake; an example is analysis 2 in table 1.

**Tg** **Gabbro (Miocene and Oligocene)**—Coarse, commonly plagioclase-phyric, sills of basaltic composition on south side of North Fork Cispus River (table 1, nos. 3, 8, and 12. May simply be coarse versions of the sills of Hugo Lake, many of which are chemically similar

**Tai** **Andesite and basaltic andesite intrusions (Miocene and Oligocene)**—Dikes, sills, and fewer small subequant hypabyssal intrusions of aphyric and one- or two-pyroxene-plagioclase-phyric basaltic andesite and andesite. Typically fine- to medium-grained and texturally resembles lava flows (map unit Ta). Sills have columnar jointing normal to contacts, quenched margins, and thicknesses of a few meters to more than 20 m. Several bodies mapped as sills in upper St John Creek area could be lava flows. Dikes characterized by subhorizontal columnar jointing, quenched margins, steep contacts with host rocks, and widths of 1–5 m. Body on Hamilton Buttes clearly cross cuts host rock and is as wide as 200 m; it has east-northeast strike similar to that of another thick dike 4.5 km farther northwest in Blue Lake quadrangle (east tip of this dike occurs just inside quadrangle.) No contact of map unit seen in quadrangle with map unit Thd, but elsewhere unit is older than the hornblende-bearing intrusions (Swanson, 1992). Probably in part feeders for flows of map unit Ta, but many dikes could be younger and have fed flows now eroded away. Compositions range from silicic basalt to mafic dacite (see numerous analyses in table 1)

## LAVA FLOWS AND VOLCANICLASTIC ROCKS

**Ttv** **Volcaniclastic rocks (Oligocene and Eocene)**—Bedded conglomerate, sandstone, siltstone, and lithic diamictite containing volcanic-derived clasts, as well as lithic- and lesser pumice-lapilli tuff and fine-grained tuff. Typically brown to buff, with the tuffaceous rocks generally green and locally white or mauve. Different rock types are interbedded at all scales, and attempts to map them separately proved unworkable. However, well-bedded sandstone dominates section in quadrangle, although lithic diamictite and tuffaceous rocks are prominent in younger part of section. Hammond (1980) and Korosec (1987) assigned unit to Ohanapecosh Formation.

Bedded epiclastic rocks range in grain size from silt to gravel (dominantly sand), in sorting and rounding from poor to good, and in bed thickness from less than 1 cm to more than 50 cm (generally a few centimeters). Sedimentary structures, such as cross bedding, channels, and both normal and inverse size grading common. Clasts are almost entirely of volcanic derivation, chiefly basaltic andesite and andesite but including more silicic rock types. Some beds low in the section are mixtures of volcanic and arkosic detritus. Fossil wood, chiefly stems and twigs, plentiful locally. Detritus probably derived by reworking of freshly erupted debris or by erosion of slightly older volcanic rocks and deposited in fluvial environment.

Clasts in lithic diamictite range in size from sand to boulders. Wide range in degree of rounding, with angular boulders commonly mixed with rounded gravel and cobbles. Thickness of single beds typically several meters but ranges from 1 m to more than 15 m. Fossil wood abundant in some beds. Commonly interbedded with fluvial sandstone, but also abundant in tuffaceous part of section. Probably mostly of debris-flow (lahar) origin.

Pumice-lapilli tuff and pumice-lithic-lapilli tuff are probably of pyroclastic-flow origin. Welding occurs but is not common. Single beds of lapilli tuff range in thickness from several meters to more than 10 m. Typically plagioclase-phyric, with minor clinopyroxene; no hornblende and rare quartz. Lithic clasts are sparse to abundant and generally andesite or dacite in composition. Fragments of charred wood are abundant in many lapilli tuffs.

Unit is almost entirely of Oligocene age in quadrangle, but air-fall tuff interbedded with middle part of arkose of Chambers Creek (map unit Tsc) yielded zircon fission-track age of 35.9 ± 0.7 Ma (Winters, 1984), late Eocene according to Cande and Kent (1992) and Odin and others (1991).

Unit locally includes andesite flows and sills too thin to map separately

**Ta** **Andesite, basaltic andesite, and basalt lava flows (Oligocene)**—Fine- to medium-grained, highly plagioclase-phyric (>20 percent) to slightly phyric (<5 percent) or even aphyric, darkly hued, lava flows and associated basal and flow-top breccia of basaltic andesite, andesite, and less common basalt. Flows typically 5–20 m thick, commonly platy and(or) columnar, with vesicular or amygdaloidal zones in many places. Phenocrysts are dominantly plagioclase, with less abundant clinopyroxene and hypersthene; most common phenocryst assemblage is plagioclase-clinopyroxene, followed by plagioclase-clinopyroxene-hypersthene and finally plagioclase-hypersthene-clinopyroxene (minerals listed in decreasing order of abundance). Groundmass texture chiefly fine-grained intersertal or intergranular, with flow-aligned microlites common; very fine-grained pilotaxitic texture characterizes more silicic rocks. Glass generally altered to clay minerals. Compositions range from basaltic andesite (table 1, no. 20) to silicic andesite (table 1, no. 61) to mafic dacite (table 1, nos. 79 and 88)). Flows of different compositions are interbedded and cannot be mapped separately short of analyzing each flow. Dikes and other intrusions of map unit Tai probably fed some flows in this unit. Interbedded extensively with volcaniclastic rocks (map unit Ttv) and includes some volcaniclastic beds too thin to map separately.

Unit mostly occurs on Goat Ridge, where flows are thermally metamorphosed to hornfels and (or) propylitically altered in many places, and epidote commonly replaces plagioclase. Flow contacts are difficult to detect in places on Goat Ridge, owing to the metamorphism, and some or all of the andesite in the extreme northeast corner of the mapped area could be part of a hypabyssal intrusion, as interpreted by Swanson and Clayton (1983)

## ARKOSE AND RELATED SEDIMENTARY ROCKS

**Tsc** **Arkose of Chambers Creek (Oligocene and Eocene)**—Well-bedded, typically micaceous arkose and subordinate pebble conglomerate, siltstone, and mudstone. Channels, cross bedding, and ripple marks common. *Chambers Creek beds* of Winters (1984), who provides thorough description of unit. Some beds are mixed with volcaniclastic detritus, and many pebbles in the conglomerate are locally derived. Interbedded with volcanic sandstone of unit Ttv. Paleocurrent directions in arkose indicate westward and southwestward river transport. Heavy mineral suite indicates provenance in moderate-grade metamorphic rocks of northern or northeastern Washington. Map portrayal is generalized and greatly simplifies complex interbedding and mixing with volcaniclastic detritus of unit Ttf

## REFERENCES CITED


Armentrout, J.M., and Suek, D.H., 1985, Hydrocarbon exploration in western Oregon and Washington: American Association of Petroleum Geologists Bulletin, v. 69, p. 627–643.

Berggren, W.A., Hilgen, F.J., Langereis, C.G., Kent, D.V., Obradovich, J.D., Raffi, Isabella, Raymo, M.E., and Shackleton, N.J., 1995, Late Neogene chronology: new perspectives in high-resoultion stratigraphy: Geological Society of America Bulletin, v. 107, p., 1272–1287.

Cande, S.C., and Kent, D.V., 1992, A new geomagnetic polarity time scale for the Late Cretaceous and Cenozoic: Journal of Geophysical Research, v. 97, p. 13,917–13,951.

Cande, S.C., and Kent, D.V., 1995, Revised calibration of the geomagnetic polarity timescale for the Late Cretaceous and Cenozoic: Journal of Geophysical Research, v. 1009, p. 6093–6095.

Church, S.E., Swanson, D.A., Williams, D.L., Clayton, G.A., Close, T.J., and Peters, T.J., 1983, Mineral resource potential of the Goat Rocks Wilderness and adjacent roadless areas, Lewis and Yakima Counties, Washington: U.S. Geological Survey Miscellaneous Field Studies Map, MF-1653-A, scale 1:48,000, 13 p.

Clayton, G.A., 1983, Geology of the White Pass area, south-central Cascade Range, Washington: Seattle, Wash., University of Washington, M.S. thesis, 212 p.

Colman, S. M., and Pierce, K. L., 1981, Weathering rinds on andesitic and basaltic stones as a Quaternary age indicator, western United States: U.S. Geological Survey Professional Paper 1210, 56 p.

Crandell, D. R., and Miller, R. D., 1974, Quaternary stratigraphy and extent of glaciation in the Mount Rainier region, Washington: U.S. Geological Survey Professional Paper 847, 59 p.

Ellingson, JA, 1959, General geology of the Cowlitz Pass area, central Cascade Mountains, Washington: Seattle, Wash., University of Washington, M.S. thesis, 60 p.

Ellingson, JA, 1968, Late Cenozoic volcanic geology of the White Pass-Goat Rocks area, Cascade Mountains, Washington: Pullman, Wash., Washington State University, Ph.D. dissertation, 112 p.

Ellingson, JA, 1972, The rocks and structure of the White Pass area, Washington: Northwest Science, v. 46, p. 9–24.

Evarts, R.C., and Ashley, R.P., 1984, Preliminary geologic map of the Spirit Lake quadrangle, Washington: U.S. Geological Survey Open-File Report 84–480, scale 1:48,000.

Evarts, R.C., and Ashley, R.P., 1990a, Preliminary geologic map of the Cougar quadrangle, Cowlitz and Clark Counties, Washington: U.S. Geological Survey Open-File Report 90–631, scale 1:24,000, 40 p.

Evarts, R.C., and Ashley, R.P., 1990b, Preliminary geologic map of the Goat Mountain quadrangle, Cowlitz County, Washington: U.S. Geological Survey Open-File Report 90–632, scale 1:24,000, 47 p.

Evarts, R.C., and Ashley, R.P., 1991, Preliminary geologic map of the Lakeview Peak quadrangle, Cowlitz County, Washington: U.S. Geological Survey Open-File Report 91–289, scale 1:24,000, 35 p.

Evarts, R.C., and Ashley, R.P., 1992, Preliminary geologic map of the Elk Mountain quadrangle, Cowlitz County, Washington: U.S. Geological Survey Open-File Report 92–362, scale 1:24,000, 44 p.

Evarts, R.C., and Ashley, R.P., 1993a, Geologic map of the Spirit Lake East quadrangle, Skamania County, Washington: U.S. Geological Survey Geologic Quadrangle Map GQ–1679, scale 1:24,000.

Evarts, R.C., and Ashley, R.P., 1993b, Geologic map of the Vanson Peak quadrangle, Lewis, Cowlitz, and Skamania Counties, Washington: U.S. Geological Survey Geologic Quadrangle Map GQ–1680, scale 1:24,000.

Evarts, R.C., and Ashley, R.P., 1993c, Geologic map of the Spirit Lake West quadrangle, Skamania and Cowlitz Counties, Washington: U.S. Geological Survey Geologic Quadrangle Map GQ–1681, scale 1:24,000.

Evarts, R.C., and Ashley, R.P., 1993d, Geologic map of the Cowlitz Falls quadrangle, Lewis and Skamania Counties, Washington: U.S. Geological Survey Geologic Quadrangle Map GQ–1682, scale 1:24,000.

Evarts, R.C., and Swanson, D.A., 1994, Geologic transect across the Tertiary Cascade volcanic arc, southern Washington, *in* Swanson, D.A., and Haugerud, R.A., eds., Geologic field trips in the Pacific Northwest: 1994 Annual Meeting, Geological Society of America, Seattle, Washington, v. 2, p.2H-1–2H-31.

Evarts, R.C., Ashley, R.P., and Smith, J.G., 1987, Geology of the Mount St. Helens area: record of discontinuous volcanic and plutonic activity in the Cascade arc of southern Washington: Journal of Geophysical Research, v. 92, p. 10,155–10,169.

Evarts, R.C., Church, S.E., and Mosier, E.L., 1983a, Mineral resource potential of the Tatoosh Roadless Area, Lewis County, Washington: U.S. Geological Survey Open-File Report 83-471, 7 p.

Evarts. R.C., Mosier, E.L., Church, S.E., and Barnes, D.J., 1983b, Mineral resource potential of the Glacier View Roadless Area, Pierce County, Washington: U.S. Geological Survey Open-File Report 83–501, 8 p.

Fiske, R.S., 1963, Subaqueous pyroclastic flows in the Ohanapecosh Formation, Washington: Geological Society of America Bulletin, v. 74, p. 391–406.

Fiske, R.S., Hopson, C.A., and Waters, A.C., 1963, Geology of Mount Rainier National Park, Washington: U.S. Geological Survey Professional Paper 444, 93 p.

Hagstrum, J.T., and Swanson, D.A., 1994, Paleomagnetism of the Miocene intrusive suite of Kidd Creek: implications for the timing of deformation in the Cascade arc, southern Washington [abs.]: Eos, American Geophysical Union, Transactions, v. 75, no. 44, p. 198–199.

Hammond, P. E., 1980, Reconnaissance geologic map and cross sections of southern Washington Cascade Range: Portland, Oregon, Publications of Department of Earth Science, scale 1:125,000.

Henriksen, D.A., 1956, Eocene stratigraphy of the lower Cowlitz River-eastern Willapa Hills area, southwestern Washington: Washington Division of Mines and Geology Bulletin 43, 122 p.

Hildreth, Wes, and Fierstein, Judy, 1995, Geologic map of the Mount Adams volcanic field, Cascade Range of southern Washington: U.S. Geological Survey Miscellaneous Geologic Investigations Map I-2460, scale 1:50,000.

Hildreth, Wes, and Lanphere, M.A. 1994, Potassium-argon geochronology of a basalt-andesite-dacite arc system: the Mount Adams volcanic field, Cascade Range of southern Washington: Geological Society of America Bulletin, v. 106, p. 1413–1429.

Irvine, T.N., and Baragar, W.R.A., 1971, A guide to the chemical classification of the common igneous rocks: Canadian Journal of Earth Sciences, v. 8, p. 523–548.

Izett, G.A., and Obradovich, J.D., 1994, $^{40}Ar/^{39}Ar$ age constraints for the Jaramillo Normal Subchron and the Matuyama-Brunhes geomagnetic boundary: Journal of Geophysical Research, v. 99, p. 2925–2934.

Johnson, S.Y., and O'Connor, J.T., 1994, Stratigraphy, sedimentology, and provenance of the Raging River Formation (early? and middle Eocene), King County, Washington: U.S. Geological Survey Bulletin 2085-A, 33 p.

Johnson, S.Y., and Stanley, W.D., 1995, Eocene paleogeography of the Morton anticline area, southwestern Washington, *in* Fritsche, A.E., ed., Cenozoic paleogeography of the western United States—II: Pacific Section, SEPM (Society for Sedimentary Geology), book 75, p. 291–309.

Korosec, M.A., 1987, Geologic map of the Mount Adams quadrangle, Washington: Washington Division of Geology and Earth Resources Open-File Report 87–5, 39 p.

Kuenzi, W.D., Horst, O.H., and McGehee, R.V., 1979, Effect of volcanic activity on fluvial-deltaic sedimentation in a modern arc-trench gap, southwestern Guatemala: Geological Society of America Bulletin, v. 90, p. 827–838.

Le Bas, M.J., Le Maitre, R.W., Streckeisen, A., and Zenettin, B., 1986, A chemical classification of volcanic rocks based on the total alkali-silica diagram: Journal of Petrology, v. 27, p. 745–750.

Marso, J.N., and Swanson, D.A., 1992, The intrusive suite of Kidd Creek: a middle Miocene magmatic event in the Cascade arc of southern Washington [abs.]: Geological Society of America Abstracts with Programs, v. 24, no. 5, p. 67.

Mattinson, J.M., 1977, Emplacement history of the Tatoosh volcanic-plutonic complex, Washington: ages of zircons: Geological Society of America Bulletin, v. 88, p. 1509–1514.

Miller, R.B., 1989, The Mesozoic Rimrock Lake inlier, southern Washington Cascades—implications for the basement to the Columbia embayment: Geological Society of America Bulletin, v. 101, p. 1289–1305.

Miller, R.B., Mattinson, J.M., Funk, S.A.G., Hopson, C.A., and Treat, C.L., 1993, Tectonic evolution of Mesozoic rocks in the southern and central Washington Cascades, *in* Dunne, G.C., and McDougall, K., eds., Mesozoic paleogeography of the western United States—II: Pacific Section, Society of Economic Paleontologists and Mineralogists, Book 71, p. 81–98.

Moore, R.B., Thornber, C.R., and Swanson, D.A., 1994, Preliminary geologic map of the Randle quadrangle, Cascade Range, Lewis County, Washington: U.S. Geological Survey Open-File Report 94-704, scale 1:24,000.

O'Connor, J.T., 1992, Provenance evolution for Eocene to Miocene clastic rocks of southwest Washington and northwest Oregon: Geological Society of America Abstracts with Programs, v. 24, no. 5, p. 73.

Odin, G.S., Montanari, A. Deino, A., Drake, R., Guise, P.G., Kreuzer, H., and Rex, D.C., 1991, Reliability of volcano-sedimentary biotite ages across the Eocene–Oligocene boundary (Apennines, Italy): Chemical Geology, Isotope Geoscience Section, v. 86, p. 203–224.

Roberts, A.E., 1958, Geology and coal resources of the Toledo-Castle Rock district, Cowlitz and Lewis Counties, Washington: U.S. Geological Survey Bulletin 1062, 71 p.

Smedes, H.W., and Prostka, H.J., 1972, Stratigraphic framework of the Absaroka Volcanic Supergroup in the Yellowstone National Park region: U.S. Geological Survey Professional Paper 729–C, 33 p.

Smith, J.G., 1987, New compilation geologic map of the Cascade Range in Washington: Geothermal Resources Council Transactions, v. 11, p. 309–314.

Smith, J.G., 1993, Geologic map of upper Eocene to Holocene volcanic and related rocks in the Cascade Range, Washington: U.S. Geological Survey Miscellaneous Investigations Map I–2005, scale 1:500,000, 19 p.

Stanley, W.D., Finn, Carol, and Plesha, J.L., 1987, Tectonics and conductivity structures in the southern Washington Cascades: Journal of Geophysical Research, v. 92, p. 10,179–10,193.

Stanley, W.D., Gwilliam, W.J., Latham, Gary, and Westhusing, Keith, 1992, The southern Washington Cascades conductor—a previously unrecognized thick sedimentary sequence?: American Association of Petroleum Geologists Bulletin, v. 76, p. 1569–1585.

Stine, C.M., 1987, Stratigraphy of the Ohanapecosh Formation north of Hamilton Buttes, south-central Washington: Portland, Oreg., Portland State University, M.S. thesis, 83 p

Swanson, D.A., 1978, Geologic map of the Tieton River area, Yakima County, south-central Washington: U.S. Geological Survey Miscellaneous Field Studies Map MF–968, scale 1:48,000.

Swanson, D.A., 1989, Geologic maps of the French Butte and Greenhorn Buttes quadrangles, Washington: U.S. Geological Survey Open-File Report 89–309, scale 1:24,000, 25 p.

Swanson, D.A., 1991, Geologic map of the Tower Rock quadrangle, southern Cascade Range, Washington: U.S. Geological Survey Open-File Report 91–314, scale 1:24,000, 26 p.

Swanson, D.A., 1992, Geologic map of the McCoy Peak quadrangle, southern Cascade Range, Washington: U.S. Geological Survey Open-File Report 92–336, scale 1:24,000, 36 p.

Swanson, D.A., 1993, Geologic map of the Blue Lake quadrangle, southern Cascade Range, Washington: U.S. Geological Survey Open-File Report 93–297, scale 1:24,000, 34 p.

Swanson, D.A., 1994a, Geologic map of the East Canyon Ridge quadrangle, southern Cascade Range, Washington: U.S. Geological Survey Open-File Report 94–591, 31 p.

Swanson, D.A., 1994b, Coeval volcanism and subsidence about 36 million years ago in the Cascade arc, southern Washington [abs.]: Geological Society of America Abstracts with Programs, v. 26, no. 7, p.A-113.

Swanson, D.A., and Clayton, G.A., 1983, Generalized geologic map of the Goat Rocks Wilderness and adjacent RARE II areas, Washington: U.S. Geological Survey Open-File Report 83-357, 5 p.

Swanson, D.A., and Evarts, R.C., 1992, Tertiary magmatism and tectonism in an E–W transect across the Cascade arc in southern Washington [abs.]: Geological Society of America Abstracts with Programs, v. 24, no. 5, p. 84.

Vance, J.A., 1989, Detrital kyanite and zircon: provenance and sediment dispersal in the middle and late Eocene Puget and Cowlitz Groups, SW Washington and NW Oregon: Geological Society of America Abstracts with Programs, v. 21, no. 5, p. 153.

Vance, J.A., Clayton, G.A., Mattinson, J.M., and Naeser, C.W., 1987, Early and middle Cenozoic stratigraphy of the Mount Rainier–Tieton River area, southern Washington Cascades: Washington Division of Geology and Earth Resources Bulletin 77, p. 269–290.

Vessell, R.K., and Davies, D.K., 1981, Nonmarine sedimentation in an active fore-arc basin, *in* Ethridge, F.G., ed., Recent and ancient nonmarine depositional environments: models for exploration: Society of Economic Paleontologists and Mineralogists Special Paper 31, p. 31–45.

Waters, A.C., 1961, Keechelus problem, Cascade Mountains, Washington: Northwest Science, v. 35, p. 39–57.

Walsh, T.J., Korosec, M.A., Phillips, W.M., Logan, R.L., and Schasse, H.W., 1987, Geologic map of Washington—southwest quadrant: Washington Division of Geology and Earth Resources Geologic Map GM-34, scale 1:250,000, 28 p.

Wells, R.E., and others, 1993, CASCADIA: Regional lithospheric studies of the Pacific Northwest: U.S. Geological Survey Open-File Report 93- 706, 39 p.

Winters, W.J., 1984, Stratigraphy and sedimentology of Paleogene arkosic and volcaniclastic strata, Johnson Creek–Chambers Creek area, southern Cascade Range, Washington: Portland, Oreg., Portland State University, M.S. thesis, 162 p.

Wright, T.L., 1960, The mineralogy and petrogenesis of the southern part of the Tatoosh pluton, Mount Rainier National Park, Washington: Baltimore, The Johns Hopkins University, Ph.D. Dissertation, 185 p.

Yamaguchi, D.K., 1985, Tree-ring evidence for a two-year interval between recent prehistoric explosive eruptions of Mount St. Helens: Geology, v. 13, p. 554–557.

# CORRELATION OF MAP UNITS

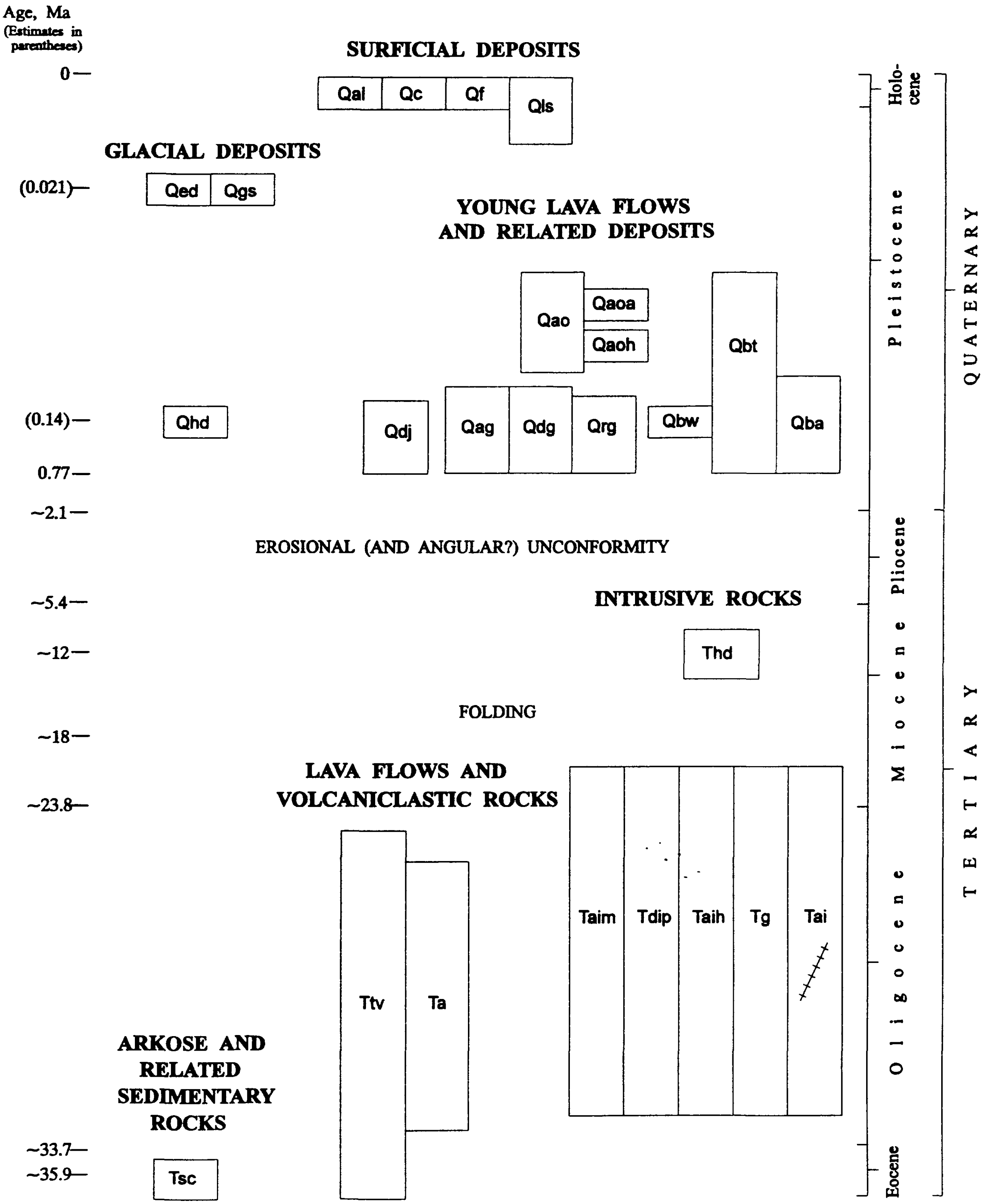

## EXPLANATION OF MAP SYMBOLS


Contact, dashed where approximately located, queried where uncertain, dotted where concealed


Contact between landslides along Wobbly Creek

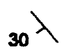

Strike and dip of bedding and flow contacts

Folds, dashed where approximately located, dotted where concealed

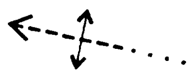
Trace of axis of anticline, showing direction of plunge


Trace of axis of syncline, showing direction of plunge

Faults, dashed where approximately located, dotted where concealed, queried where uncertain


High-angle fault; bar and ball on downthrown side if known

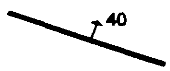

Direction and magnitude of dip of fault plane


Fault or shear zone; arrows indicate sense of lateral displacement

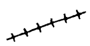
Dike of andesite and basaltic andesite of units Ta, Taih, and Tai

Site of chemically analyzed sample, with map number. Number refers to table 1

| | |
|---|---|
| 1 ▼ | Basalt |
| 26 ▲ | Basaltic andesite |
| 53 △ | Andesite |
| 85 ○ | Dacite |
| 93 ● | Rhyolite |

◆1A Site of zircon fission-track age from Winters (1984) and discussed in text